

Power law distribution of seismic rates: theory and data

A. Saichev^{1,2} and D. Sornette^{3,4}

¹*Mathematical Department, Nizhny Novgorod State University,
Gagarin prosp. 23, Nizhny Novgorod, 603950, Russia*

²*Institute of Geophysics and Planetary Physics,
University of California, Los Angeles, CA 90095*

³*Institute of Geophysics and Planetary Physics and Department of Earth and Space Sciences,
University of California, Los Angeles, CA 90095*

⁴*Laboratoire de Physique de la Matière Condensée,
CNRS UMR 6622 and Université de Nice-Sophia Antipolis, 06108 Nice Cedex 2, France**

(Dated: September 4, 2018)

Abstract

We report an empirical determination of the probability density functions $P_{\text{data}}(r)$ of the number r of earthquakes in finite space-time windows for the California catalog, over fixed spatial boxes $5 \times 5 \text{ km}^2$ and time intervals $dt = 1, 10, 100$ and 1000 days. We find a stable power law tail $P_{\text{data}}(r) \sim 1/r^{1+\mu}$ with exponent $\mu \approx 1.6$ for all time intervals. These observations are explained by a simple stochastic branching process previously studied by many authors, the ETAS (epidemic-type aftershock sequence) model which assumes that each earthquake can trigger other earthquakes (“aftershocks”). An aftershock sequence results in this model from the cascade of aftershocks of each past earthquake. We develop the full theory in terms of generating functions for describing the space-time organization of earthquake sequences and develop several approximations to solve the equations. The calibration of the theory to the empirical observations shows that it is essential to augment the ETAS model by taking account of the pre-existing frozen heterogeneity of spontaneous earthquake sources. This seems natural in view of the complex multi-scale nature of fault networks, on which earthquakes nucleate. Our extended theory is able to account for the empirical observation satisfactorily. In particular, the adjustable parameters are determined by fitting the largest time window $dt = 1000$ days and are then used as frozen in the formulas for other time scales, with very good agreement with the empirical data.

*Electronic address: sornette@moho.ess.ucla.edu

I. INTRODUCTION

Many papers purport to characterize the space-time organization of seismicity in different regions of the world. Recent claims of universal laws for the distribution of waiting times and seismic rates between earthquakes have derived from the analyses of space-time windows [1, 2]. The flurry of interest from physicists comes from their fascination with the self-similar properties exhibited by seismicity (Gutenberg-Richter power law of earthquake seismic moments, Omori decay law of aftershock rates, fractal and multifractal space-time organization of earthquakes and faults) together with the development of novel concepts and techniques that may provide new insights [3, 4, 5, 6, 7].

The interest is no less vivid among seismologists and geophysicists in characterizing the space-time properties of seismicity, because it allows them to understand the dynamics of plate motion (at large scales), to constrain the interaction between faults, as well as to develop better hazard assessment. Recently, an additional incentive is provided by the development of forecasting models of seismicity, for instance within the RELM (Regional Earthquake Likelihood Models: www.relm.org) project in Southern California. In the RELM project, a forecast is expressed as a vector of earthquake rates specified for each multi-dimensional bin [8], where a bin is defined by an interval of location, time, magnitude and focal mechanism and the resolution of a model corresponds to the bin sizes. Then, expectations and likelihoods can be estimated and used for the comparison between different forecasting methods.

A fundamental issue is testing models' prediction is to take into account so-called aftershock clustering. In one way or another, most if not all models use some form of declustering approach to remove the effect of aftershocks which otherwise dominate and obscure the desired information about the model's performance [8]. Then, with such declustered catalogs, the likelihood of forecasts are estimated using Poissonian probabilities. But, if the catalog is only partially declustered (which it will most probably be as there are no agreed upon fully efficient method of declustering), then our contribution in this paper is to show that the distribution of event numbers should present a tail much more heavy than predicted by the Poissonian statistics and to propose a theoretical explanation for it. Pisarenko and Golubeva [9] introduced a model to decluster catalogs by so-to-say Poisson "with random parameter," which resulted in a law with slowly decreasing probabilities (actually a stable Lévy law) for the distribution of rates.

We improve on preceding results on several points. Our first contribution is to show that the heavy tail nature of the distribution of seismic rate is intrinsic to a class of generic models of triggered seismicity. Specifically, our theory is based on a simple model of earthquake triggering, in which future seismicity is a conditional Poisson process, with average rates (or Poisson intensity) conditioned on past seismicity. We show that the exponential Poisson rate is renormalized into a power law tail by the mechanism involving a cascade of earthquake triggering. Our theory thus provides a prediction for the distribution of seismic rates in space-time bins in the form of a power law tail distribution. Our second contribution is to show that our prediction is verified by empirical seismic rates in Southern California over more than two decades. In addition, our theory accounts well for the evolution of the distribution of seismic rates as a function of the time window size from 1 day to 1000 days.

This implies that spontaneous fluctuations of the number of triggered earthquakes in space-time bins may be simply due to the cascades of triggering processes, which lead to dramatic departures from the Poisson model used as one of the building block of standard testing procedures. Accounting for the intrinsic heavy tail nature of the distribution of seismic rate may explain, we believe, many of the contradictions and rejections of models assessed on the basis of Poisson statistics of so-called declustered catalogs. This also suggests the need for fundamentally different earthquake prediction models and testing methods. Our results also offer a simple alternative explanation to so-called universal laws [1, 2] in terms of cascades of triggered earthquakes: our proposed framework explains the observed power law distributions of seismic rates from the fundamentals of seismicity characterized by a few exponents.

II. THE EPIDEMIC-TYPE AFTERSHOCK SEQUENCE (ETAS) BRANCHING MODEL OF EARTHQUAKES WITH LONG MEMORY

We study the general branching process, called the Epidemic-Type Aftershock Sequence (ETAS) model of triggered seismicity, introduced by Ogata in the present form [10] and by Kagan and Knopoff in a slightly different form [11] and whose main statistical properties are reviewed in [12]. For completeness and in order to fix notations, we recall its definition and ingredients used in our analysis that follows. In this model, all earthquakes are treated on the same footing and there is no distinction between foreshocks, mainshocks and aftershocks, other than from retrospective

human-made classification. The advantage of the ETAS model is its conceptual simplicity based on three independent well-found empirical laws and its power of explanation of other empirical observations (see for instance [13] and references therein).

The ETAS model belongs to a general class of branching processes [14, 15], and has in addition the property that the variance of the number of earthquake progenies triggered in direct lineage from a given mother earthquake is mathematically infinite. Moreover, a long-time (power law) memory of the impact of a mother on her first-generation daughters describes the empirical Omori law for aftershocks. These two ingredients together with the mechanism of cascades of branching have been shown to give rise to subdiffusion [16, 17] and to non mean-field behavior in the distribution of the total number of aftershocks per mainshock, in the distribution of the total number of generations before extinctions [18] and in the distribution of the total duration of an aftershock sequence before extinction [19].

In the ETAS model, each earthquake is a potential progenitor or mother, characterized by its conditional average number

$$N_m \equiv \kappa \mu(m) \quad (1)$$

of children (triggered events or aftershocks of first generation), where

$$\mu(m) = 10^{\alpha(m-m_0)} , \quad (2)$$

is a mark associated with an earthquake of magnitude $m \geq m_0$ (in the language of “marked point processes”), κ is a constant factor and m_0 is the minimum magnitude of earthquakes capable of triggering other earthquakes. The meaning of the term “conditional average” for N_m is the following: for a given earthquake of magnitude m and therefore of mark $\mu(m)$, the number r of its daughters of first generation are drawn at random according to the Poissonian statistics

$$p_\mu(r) = \frac{N_m^r}{r!} e^{-N_m} = \frac{(\kappa \mu)^r}{r!} e^{-\kappa \mu} . \quad (3)$$

N_m is the expectation of the number of daughters of first generation, conditioned on a fixed magnitude m and mark $\mu(m)$. The expression (2) for $\mu(m)$ is chosen in such a way that it reproduces the empirical dependence of the average number of aftershocks triggered directly by an earthquake of magnitude m (see [20] and references therein). Expression (1) with (2) gives the so-called productivity law of a given mother as a function of its magnitude. The challenge of our

present analysis is to understand how the exponential distribution (3) is changed by taking into account all earthquake triggering paths simultaneously and at all possible generations.

The ETAS model is complemented by the Gutenberg-Richter (GR) density distribution of earthquake magnitudes

$$p(m) = b \ln(10) 10^{-b(m-m_0)} , \quad m \geq m_0 , \quad (4)$$

such that $\int_m^\infty p(x)dx$ gives the probability that an earthquake has a magnitude equal to or larger than m . This magnitude distribution $p(m)$ is assumed to be independent of the magnitude of the triggering earthquake, i.e., a large earthquake can be triggered by a smaller one [13, 20].

Combining (4) and (2) shows that the earthquake marks μ and therefore the conditional average number N_m of daughters of first generation are distributed according to the normalized power law

$$p_\mu(\mu) = \frac{\gamma}{\mu^{1+\gamma}} , \quad 1 \leq \mu < +\infty, \quad \gamma = b/\alpha . \quad (5)$$

For earthquakes, $b \approx 1$ and $0.5 < \alpha < 1$ giving $1 < \gamma < 2$ (see [21] for a review of values quoted in the literature and their implications). This range $1 < \gamma < 2$ implies that the mathematical expectation of μ and therefore of N_m (performed over all possible magnitudes) is finite but its variance is infinite (the marginal case $\alpha = 1$ leading to $\gamma = 1$ requires the existence of an upper magnitude cut-off [21]).

For a fixed γ , the coefficient κ then controls the value of the average number n (or branching ratio) of children of first generation per mother:

$$n = \langle N_m \rangle = \kappa \langle \mu \rangle = \kappa \frac{\gamma}{\gamma - 1} , \quad (6)$$

where the average $\langle N_m \rangle$ is taken over all mothers' magnitudes drawn from the GR law. Recall that the values $n < 1$, $n = 1$ and $n > 1$ correspond respectively to the sub-critical, critical and super-critical regimes.

The next ingredient of the ETAS model consists in the specification of the space-time rate function $N_m \Phi(\mathbf{r} - \mathbf{r}_i, t - t_i)$ giving the average rate of first generation daughters at time t and position \mathbf{r} created by a mother of magnitude $m \geq m_0$ occurring at time t_i and position \mathbf{r}_i :

$$\Phi(\mathbf{x}, t) = \Phi(t) \phi(\mathbf{x}) . \quad (7)$$

The time propagator $\Phi(t)$ has the Omori law form

$$\Phi(t) = \frac{\theta c^\theta}{(c + t)^{1+\theta}} H(t) \quad (8)$$

where $H(t)$ is the Heaviside function, $0 < \theta < 1$, c is a regularizing time scale that ensures that the seismicity rate remains finite close to the mainshock. The time decay rate (8) is called the “direct Omori law” [12, 22]. Due to the process of cascades of triggering by which a mother triggers daughters which then trigger their own daughters and so on, the direct Omori law (8) is renormalized into a “dressed” or “renormalized” Omori law [12, 22], which is the one observed empirically. The analysis below will retrieve and extend this result.

The space propagator is given by

$$\phi(\mathbf{x}) = \frac{\eta d^\eta}{2\pi(x^2 + d^2)^{(\eta+2)/2}}. \quad (9)$$

For our comparison with the empirical data, we shall consider the epicenter position of earthquakes, that is, the 2D-projection on the earth surface of the real 3D-distribution of earthquake hypocenters. Numerical implementations of the theory developed below will thus be done in 2D but it is easy to generalize to 3D if/when the empirical data will be of sufficient quality to warrant it.

In the following, we will make use of the Laplace transform of the Omori law

$$\hat{\Phi}(u) = \int_0^\infty \Phi(t) e^{-ut} dt = \theta (cu)^\theta e^{cu} \Gamma(-\theta, cu) \quad (10)$$

and of its asymptotic behavior

$$\hat{\Phi}^{-1}(u) \sim 1 + \Gamma(1 - \theta)(cu)^\theta, \quad cu \ll 1. \quad (11)$$

The Fourier transform of the space propagator (9) will also be useful:

$$\tilde{\phi}(\mathbf{q}) = \iint_{-\infty}^{\infty} \phi(\mathbf{x}) e^{i(\mathbf{q} \cdot \mathbf{x})} d\mathbf{x} = 2 \left(\frac{dq}{2} \right)^{\eta/2} \frac{K_{\eta/2}(dq)}{\Gamma(\eta/2)} \quad (12)$$

In particular

$$\tilde{\phi}(\mathbf{q}) = e^{-dq} \quad (\eta = 1), \quad \tilde{\phi}(\mathbf{q}) = e^{-dq}(1 + dq) \quad (\eta = 3). \quad (13)$$

The last ingredient of the ETAS model is to assume that plate tectonic motion induces spontaneous mother earthquakes, which are not triggered by previous earthquakes, according to a Poissonian point process, such that the average number of spontaneous mother earthquakes per unit time and per unit surface is ρ . In the ETAS branching model, each such spontaneous mother earthquake then triggers independently its own space-time aftershocks branching process.

It is a well-established fact that, at large scale, earthquakes are preferentially clustered near the plate boundaries while, at smaller scales, earthquakes are found mostly along faults and close to nodes between several faults [23]. It is natural to extend the ETAS model to allow for the heterogeneity of the spontaneous earthquake sources ϱ reflecting the influence of pre-existing fault structures, some rheological heterogeneity and complex spatial stress distributions. We get some guidelines from the distribution of the stress field in heterogeneous media and due to earthquakes [24] which should be close to a Cauchy distribution or probably more generally to a power law [25, 26] (see also Chap. 17 of [27]).

The simplest prescription is thus to assume that ϱ is itself random and distributed according to

$$\frac{1}{\langle \varrho \rangle} f\left(\frac{\varrho}{\langle \varrho \rangle}\right), \quad (14)$$

where $\langle \varrho \rangle$ is then statistical average of the random space-time Poissonian source intensity ϱ . In the numerical applications below, we shall use the form

$$f_\delta(x) = \frac{\delta + 1}{\delta} \left(1 + \frac{x}{\delta}\right)^{-2-\delta} \quad (\delta > 0), \quad (15)$$

The value $\delta = 0$ gives the same tail as the Cauchy distribution advocated in [24] for the stress field. We have considered other functions, such as half-Gaussian, exponential, half-Cauchy but none of them give satisfactory fits to the data (see below). The parametrization (15) with $\delta > 0$ allows us to have only a single scale $\langle \varrho \rangle$ controlling the typical fluctuation of the random sources. We have found that only slightly positive values of δ (corresponding to tails a little fatter than the Cauchy law) gives reasonable fits to the data (see below). It is interesting to observe that the data on the distribution of seismic rates thus seems to constrain significantly the fractal distribution of seismic sources.

III. GENERATING PROBABILITY FUNCTION (GPF) OF EARTHQUAKES BRANCHING PROCESS

In this section, we describe the statistical properties of earthquake branching processes using the technology of generating functions.

First, let us recall the GPF of the total number R_1 of the first-generation aftershocks of a mother

event of magnitude m can be easily obtained as

$$e^{\mu\kappa(z-1)}, \quad (16)$$

using the fact that the rate of first-generation aftershocks is Poissonian according to (3). In this expression (16), κ and μ are given by their definition in (1) and (2).

Averaging (16) over the random parameter μ gives the GPF of the number R_1 of first generation aftershocks triggered by a mother aftershock of arbitrary magnitude

$$G(z) = \gamma\kappa^\gamma(1-z)^\gamma \Gamma(-\gamma, \kappa(1-z)). \quad (17)$$

Note that $\langle R_1 \rangle$ is nothing but the branching ratio n defined above in equation (6). Knowing the expression (17) for the GPF $G(z)$, one finds that the corresponding probabilities of the random numbers R_1 are equal to

$$P_1(r) = \Pr\{R_1 = r\} = \gamma \frac{\kappa^\gamma}{r!} \Gamma(r - \gamma, \kappa), \quad (18)$$

which have the following asymptotics

$$P_1(r) \simeq \frac{\gamma\kappa^\gamma}{r^{\gamma+1}} = n^\gamma \gamma^{1-\gamma} (\gamma - 1)^\gamma r^{-\gamma-1} \quad (r \gg 1). \quad (19)$$

Expression (19) implies that, for $1 < \gamma < 2$, the variance of the random number R_1 is infinite. For $\gamma > 2$, the variance is finite and is equal to

$$\sigma_1^2 = \frac{n^2}{\gamma(\gamma - 2)} + n. \quad (20)$$

Figure 1 shows the probabilities (18) and their power law asymptotics for $n = 1$, $\gamma = 1.25$ and $\gamma = 3$.

Let us now consider the set of independent space-time aftershock branching processes, triggered by spontaneously arising mother earthquakes. Due to the independence between each sequence triggered by each spontaneous event, it is easy to show that the GPF of the number of events (including mother earthquakes and all their aftershocks of all generations), falling into the space-time window $\{[t, t + \tau] \times \mathcal{S}\}$ is equal to

$$\Theta_{\text{sp}}(z, \tau, \mathcal{S}) = e^{-\varrho L(z, \tau, \mathcal{S})} \quad (21)$$

where

$$\begin{aligned}
L(z, \tau, \mathcal{S}) = & \int_0^\infty dt \iint_{-\infty}^\infty d\mathbf{x} [1 - \Theta(z, t, \tau, \mathcal{S}; \mathbf{x})] + \\
& \int_0^\tau dt \iint_{-\infty}^\infty d\mathbf{x} [1 - \Theta(z, t, \mathcal{S}; \mathbf{x})][1 - I_{\mathcal{S}}(\mathbf{x})] + \\
& \int_0^\tau dt \iint_{\mathcal{S}} d\mathbf{x} [1 - z\Theta(z, t, \mathcal{S}; \mathbf{x})].
\end{aligned} \tag{22}$$

The three above summands have the following transparent geometrical meaning.

- The first summand describes the contribution to the GPF Θ_{sp} from aftershocks triggered by mother earthquakes that occurred before the time window (i.e. at instants t' such that $t' < t$) (positions 1 in Fig. 2). The corresponding GPF $\Theta(z, t - t', \tau, \mathcal{S}; \mathbf{x})$ of the number of aftershocks triggered inside the space-time window $\{[t, t + \tau] \times \mathcal{S}\}$ by some mother event that occurred at time t' satisfies the relation

$$\Theta(z, t, \tau, \mathcal{S}; \mathbf{x}) = G[1 - \Psi(z, t, \tau, \mathcal{S}; \mathbf{x})], \tag{23}$$

where the auxiliary function $\Psi(z, t, \tau, \mathcal{S}; \mathbf{x})$, describing the space-time dissemination of aftershocks triggering by some mother event, is equal to

$$\begin{aligned}
\Psi(z, t, \tau, \mathcal{S}; \mathbf{x}) = & \\
& \Phi(\mathbf{x}, t) \otimes [1 - \Theta(z, t, \tau, \mathcal{S}; \mathbf{x})] + \Phi(\mathbf{x}, t + \tau) \otimes [1 - \Theta(z, \tau, \mathcal{S}; \mathbf{x})] + \\
& (1 - z)\Phi(\mathbf{x}, t + \tau) \otimes I_{\mathcal{S}}(\mathbf{x})\Theta(z, \tau, \mathcal{S}; \mathbf{x}).
\end{aligned} \tag{24}$$

$\Phi(\mathbf{x} - \mathbf{x}', t')$, which has been defined in (7), is the probability density function (pdf) of the position \mathbf{x}' and instant t' of some first generation aftershock, triggered by the mother event, arising at the instant $t = 0$ and at the point \mathbf{x} . The function $I_{\mathcal{S}}(\mathbf{x})$ in (24) is the indicator of the space window \mathcal{S} and $G(z)$ in (23) is the GPF of the number R_1 of first generation aftershocks, triggered by some mother earthquake. $G(z)$ given in (17) is common to all mother earthquakes and to all aftershocks.

- The last two terms in expression (22) (positions 2 and 3 in Fig. 2) describe the contribution of aftershocks triggered by earthquakes, occurring inside the time window (i.e., $t' \in [t, t + \tau]$). The second term (position 2 in Fig. 2) corresponds to the subset spatially outside the domain

\mathcal{S} . The third term (position 3 in Fig. 2) corresponds to the subset spatially inside the domain \mathcal{S} . These last two terms in expression (22) depend on the GPF

$$\Theta(z, \tau, \mathcal{S}; \mathbf{x}) = \Theta(z, t = 0, \tau, \mathcal{S}; \mathbf{x}) \quad (25)$$

of the numbers of aftershocks triggered till time τ inside the space window \mathcal{S} by some mother event arising at the instant $t = 0$ and at the point \mathbf{x} . It follows from (23) and (24) that it satisfies the relations

$$\Theta(z, \tau, \mathcal{S}; \mathbf{x}) = G[1 - \Psi(z, \tau, \mathcal{S}; \mathbf{x})] \quad (26)$$

and

$$\begin{aligned} \Psi(z, \tau, \mathcal{S}; \mathbf{x}) = \\ \Phi(\mathbf{x}, \tau) \otimes [1 - \Theta(z, \tau, \mathcal{S}; \mathbf{x})] + (1 - z)\Phi(\mathbf{x}, \tau) \otimes I_{\mathcal{S}}(\mathbf{x})\Theta(z, \tau, \mathcal{S}; \mathbf{x}). \end{aligned} \quad (27)$$

In addition, we shall need the GPF

$$\Theta(z, \mathcal{S}; \mathbf{x}) = \Theta(z, \tau = \infty, \mathcal{S}; \mathbf{x}) \quad (28)$$

of the total numbers of aftershocks triggered by some mother earthquake inside the area \mathcal{S} . As seen from (26) and (27), it satisfies the relations

$$\Theta(z, \mathcal{S}; \mathbf{x}) = G[1 - \Psi(z, \mathcal{S}; \mathbf{x})] \quad (29)$$

and

$$\Psi(z, \mathcal{S}; \mathbf{x}) = 1 - \phi(\mathbf{x}) \otimes \Theta(z, \mathcal{S}; \mathbf{x}) + (1 - z)\phi(\mathbf{x}) \otimes I_{\mathcal{S}}(\mathbf{x})\Theta(z, \mathcal{S}; \mathbf{x}). \quad (30)$$

Taking into account the distribution of the source intensities ϱ amounts to averaging equation (21) over ϱ weighted with the statistics (14). This gives

$$\Theta_{\text{sp}}(z, \tau; \mathcal{S}) = \hat{f}[\langle \varrho \rangle L(z, \tau, \mathcal{S})], \quad (31)$$

where $\hat{f}(u)$ is the Laplace transform of the pdf $f(x)$. For the specification (15), expression (31) becomes

$$\hat{f}_{\delta}(u) = (1 + \delta)(\delta u)^{1+\delta} e^{\delta u} \Gamma(-1 - \delta, \delta u). \quad (32)$$

IV. AVERAGES AND RATES OF AFTERSHOCKS WITHIN THE SPACE-TIME WINDOW $\{[t, t + \tau] \times \mathcal{S}\}$

Before discussing the properties of the distributions of aftershocks, we consider their simplest statistical characteristics, namely the averages and rates of different kinds of aftershocks. This introduces the relevant characteristic scales in the time and in the space domains, which are found inherent to the space-time branching processes. This also suggests the natural “large time window approximation” used and tested below within the more general probabilistic treatment.

A. Average of the total number of events in the space time window $\{[t, t + \tau] \times \mathcal{S}\}$

Let us first calculate the average the total number of events inside the space-time window given by

$$\langle R_{\text{sp}}(\tau, \mathcal{S}) \rangle = \left. \frac{\partial \Theta_{\text{sp}}(z, \tau, \mathcal{S})}{\partial z} \right|_{z=1}. \quad (33)$$

It follows from (31) and (22) that it is equal to

$$\langle R_{\text{sp}}(\tau, \mathcal{S}) \rangle = \langle R_{\text{out}}(\tau, \mathcal{S}) \rangle + \langle R(\tau, \mathcal{S}) \rangle + \langle \varrho \rangle S \tau, \quad (34)$$

where $\langle R_{\text{out}}(\tau, \mathcal{S}) \rangle$ is the average number of aftershocks triggered by spontaneous “mother” earthquake sources that occurred before time t (positions 1 in Fig. 2), $\langle R(\tau, \mathcal{S}) \rangle$ is the average of number of aftershocks triggering by spontaneous earthquake sources that occur within the time interval $[t, t + \tau]$ (positions 2 and 3 in Fig. 2) and $\langle \varrho \rangle S \tau$ is the average of number of spontaneous earthquakes inside the space-time window. Here and everywhere in the following, S is the area of the spatial domain \mathcal{S} and thus $S \tau$ is the space-time volume associated with the space-time window.

In what follows, it will be useful to introduce the rate of events

$$N_{\text{sp}}(\tau, \mathcal{S}) = \frac{d \langle R_{\text{sp}}(\tau, \mathcal{S}) \rangle}{d \tau}, \quad (35)$$

with

$$N_{\text{sp}}(\tau, \mathcal{S}) = N_{\text{out}}(\tau, \mathcal{S}) + N(\tau, \mathcal{S}) + \langle \varrho \rangle S. \quad (36)$$

Using Eq. (23), (24) and Eq. (26), (27), one shows that

$$N(\tau, \mathcal{S}) = \frac{n}{1 - n} \langle \varrho \rangle S - N_{\text{out}}(\tau, \mathcal{S}). \quad (37)$$

where $N_{\text{out}}(\tau, \mathcal{S})$ satisfies the equation

$$N_{\text{out}}(\tau, \mathcal{S}) - n N_{\text{out}}(\tau, \mathcal{S}) \otimes \Phi(\tau) = \frac{n \langle \varrho \rangle S}{1 - n} a(\tau), \quad (38)$$

and n is the branching ratio defined in (6). Here and below, the following notation is used

$$a(\tau) = \int_{\tau}^{\infty} \Phi(t) dt = \left(\frac{c}{\tau + c} \right)^{\theta}. \quad (39)$$

Substituting (37) into (36) gives the obvious equality

$$N_{\text{sp}}(\tau, \mathcal{S}) = \frac{\langle \varrho \rangle S}{1 - n}, \quad (40)$$

which implies that, due to the cascade of earthquake triggering processes, the average of the total number $\langle R_{\text{sp}}(\tau, \mathcal{S}) \rangle$ of events is amplified by the factor $1/(1 - n)$ compared with the average number $\langle \varrho \rangle \tau S$ of earthquake sources. This factor $1/(1 - n)$ has a simple intuitive meaning [28]: one event gives on average n daughters in direct lineage; each of these first-generation daughters give n grand-daughters, the average number of grand-daughters is thus n^2 , and the reasoning continues over all generations. Summing over all generations, the total number of events triggered by a given source plus the source itself is $1 + n + n^2 + n^3 + \dots$, which sums to $1/(1 - n)$.

B. Impact of mother earthquake sources occurring before the time window

Here, we use previous and other related relations in the goal of estimating the contribution of the different terms in the r.h.s. of Eq. (22) to the GPF $\Theta_{\text{sp}}(z, \tau, \mathcal{S})$. Our goal is to prepare and check for approximations that will be used below.

For instance, we shall assume that the contribution of the first term in (22), which is responsible for aftershocks triggered by earthquakes occurring before time t (i.e., outside the time window $[t, t + \tau]$), is negligible if the corresponding relative events rate obeys the following condition

$$\mathcal{N}_{\text{out}}(\tau) = \frac{N_{\text{out}}(\tau, \mathcal{S})}{N_{\text{sp}}(\tau, \mathcal{S})} \ll 1. \quad (41)$$

To check when this condition holds, notice that, due to (38), (40), $\mathcal{N}_{\text{out}}(\tau)$ is solution of

$$\mathcal{N}_{\text{out}}(\tau) - n \mathcal{N}_{\text{out}}(\tau) \otimes \Phi(\tau) = n a(\tau). \quad (42)$$

Applying the Laplace transform to both sides of this equation gives

$$\hat{\mathcal{N}}_{\text{out}}(u) = n \frac{1 - \hat{\Phi}(u)}{u[1 - n\hat{\Phi}(u)]}. \quad (43)$$

Using the asymptotic formula (11), we obtain

$$\hat{\mathcal{N}}_{\text{out}}(u) \simeq \frac{n (c_1 u)^{\theta-1}}{1 + (c_1 u)^\theta}, \quad (44)$$

where

$$c_1 = \left(\frac{\Gamma(1-\theta)}{1-n} \right)^{1/\theta} c \quad (45)$$

is a characteristic time-scale of aftershock branching processes separating a $1/t^{1-\theta}$ law at $t < c_1$ from a $1/t^{1+\theta}$ law at $t > c_1$ for the decay with time of the average aftershock rate triggered by a single mother earthquake [12, 22]. For instance, if $c = 2$ min, $n = 0.9$, $\theta = 1/2$ then $c_1 \simeq 628$ min $\simeq 10.5$ hours.

Taking the inverse Laplace transform of Eq. (44) gives

$$\mathcal{N}_{\text{out}}(\tau) = n E_\theta \left[- \left(\frac{\tau}{c_1} \right)^\theta \right] \quad (46)$$

where $E_\theta(x)$ is the Mittag-Leffler function defined by

$$E_\theta(-x) = \frac{x}{\pi} \sin \pi \theta \int_0^\infty \frac{y^{\theta-1} e^{-y} dy}{y^{2\theta} + x^2 + 2xy^\theta \cos \pi \theta} \quad (x > 0, 0 < \theta < 1). \quad (47)$$

The following asymptotic property holds:

$$E_\theta(-x) \sim \frac{1}{x \Gamma(1-\theta)} \quad (x \rightarrow \infty) \quad (48)$$

In addition,

$$E_{1/2}(-x) = e^{x^2} \text{erfc } x. \quad (49)$$

Figure 3 plots the exact rate $\mathcal{N}_{\text{out}}(\tau)$, its fractional approximation (46) and corresponding asymptotics derived from (48):

$$\mathcal{N}_{\text{out}}(\tau) \simeq \frac{n}{\Gamma(1-\theta)} \left(\frac{c_1}{\tau} \right)^\theta, \quad (50)$$

for $n = 0.9$ and $\theta = 1/2$. One can observe that the asymptotic result (50) is rather precise even if τ is close to c_1 . Eq. (50) means that, if

$$\tau \gg c_1, \quad (51)$$

then one can neglect the contribution of aftershocks triggered by the spontaneous earthquake sources occurring before the time window $[t, t + \tau]$. The remark will be used in our following investigation and the condition (51) will be referred to as the “large time window approximation.”

C. Impact of mother earthquake sources occurring inside the space-time window $\{[t, t + \tau] \times \mathcal{S}\}$

Let calculate the contribution to the rate (36) of events corresponding to the last term of (22) (position 3 in Fig. 2). This term describes all the aftershocks triggered by mother earthquakes occurring within the space-time window $\{[t, t + \tau] \times \mathcal{S}\}$. It is easy to show that the corresponding seismic rate, which can be compared with the contribution (40), is equal to

$$\mathcal{N}_{\text{in}}(\tau; \mathcal{S}) = 1 - n + \frac{1 - n}{S} \iint_{\mathcal{S}} \langle R(\tau, \mathcal{S}; \mathbf{x}) \rangle d\mathbf{x}, \quad (52)$$

where

$$\langle R(\tau, \mathcal{S}; \mathbf{x}) \rangle = \left. \frac{\partial \Theta(z, \tau, \mathcal{S})}{\partial z} \right|_{z=1} \quad (53)$$

is the average number of aftershocks triggered within the space window \mathcal{S} till instant τ by some mother earthquake occurring at position \mathbf{x} and at the time $t = 0$. Using relations (26) – (30), one can show that

$$\langle R(\tau, \mathcal{S}; \mathbf{x}) \rangle = \langle R(\mathcal{S}; \mathbf{x}) \rangle - \langle R_+(\tau, \mathcal{S}; \mathbf{x}) \rangle, \quad (54)$$

where $\langle R(\mathcal{S}; \mathbf{x}) \rangle$ is the total number of aftershocks falling inside the space domain \mathcal{S} which are triggered by a earthquake source occurring at position \mathbf{x} and at the time $t = 0$. $\langle R_+(\tau, \mathcal{S}; \mathbf{x}) \rangle$ is the corresponding number of aftershocks falling with the space domain \mathcal{S} after the instant τ .

It is easy to show that the Laplace (with respect to τ) and the Fourier (with respect to \mathbf{x}) transform of $\langle R_+(\tau, \mathcal{S}; \mathbf{x}) \rangle$ is equal to

$$\langle \hat{R} \rangle_+(u, \mathcal{S}; \mathbf{q}) = n \tilde{\phi}_{\mathcal{S}}(\mathbf{q}) \frac{1}{u} \left(\frac{1}{1 - n \tilde{\phi}(\mathbf{q})} - \frac{\tilde{\Phi}(u)}{1 - n \tilde{\phi}(\mathbf{q}) \tilde{\Phi}(u)} \right), \quad (55)$$

Using the asymptotics (11), we can rewrite this last relation in the form

$$\langle \hat{R} \rangle_+(u, \mathcal{S}; \mathbf{q}) \simeq \langle \tilde{R} \rangle(\mathcal{S}; \mathbf{q}) \frac{\Gamma(1 - \theta) c^\theta u^{\theta-1}}{\Gamma(1 - \theta)(cu)^\theta + 1 - n \tilde{\phi}(\mathbf{q})}, \quad (56)$$

where $\langle \tilde{R} \rangle(\mathcal{S}; \mathbf{q})$ is the Fourier transform of the average $\langle R(\mathcal{S}; \mathbf{x}) \rangle$ of the total number of aftershocks mentioned above. Using relations (29), (30), we obtain

$$\langle \tilde{R} \rangle(\mathcal{S}; \mathbf{q}) = \frac{n \tilde{\phi}(\mathbf{q})}{1 - n \tilde{\phi}(\mathbf{q})} \tilde{I}_{\mathcal{S}}(\mathbf{q}), \quad (57)$$

where $\tilde{I}_{\mathcal{S}}(\mathbf{q})$ is the Fourier transform of the indicator function of the space window \mathcal{S} . In what follows, we assume that \mathcal{S} is the circular domain of radius ℓ centered at the origin of the plane \mathbf{x} . Then

$$\tilde{I}_{\mathcal{S}}(\mathbf{q}) = 2\pi \frac{\ell}{q} J_1(\ell q). \quad (58)$$

Eq. (56) implies that $\langle R_+(\tau, \mathcal{S}; \mathbf{x}) \rangle$ is given by

$$\langle R_+(\tau, \mathcal{S}; \mathbf{x}) \rangle = \langle R(\mathcal{S}; \mathbf{x}) \rangle \otimes \mathcal{H}(\tau; \mathbf{x}), \quad (59)$$

where the Fourier transform of the function $\mathcal{H}(\tau; \mathbf{x})$ is equal to

$$\tilde{\mathcal{H}}(\tau; \mathbf{q}) = E_{\theta} \left(-\frac{1 - n\tilde{\phi}(\mathbf{q})}{1 - n} \left(\frac{\tau}{c_1} \right)^{\theta} \right). \quad (60)$$

Thus, the Fourier transform (with respect to \mathbf{x}) of the sought average given by (54) is

$$\langle \tilde{R} \rangle(\tau, \mathcal{S}; \mathbf{q}) \simeq \langle \tilde{R} \rangle(\mathcal{S}; \mathbf{q}) \left[1 - E_{\theta} \left(-\frac{1 - n\tilde{\phi}(\mathbf{q})}{1 - n} \left(\frac{\tau}{c_1} \right)^{\theta} \right) \right]. \quad (61)$$

Using expression (61), we construct Figure 4 which plots $\langle R(\tau, \mathcal{S}; \mathbf{x}) \rangle$ for different values of τ/c_1 , in order to illustrate its convergence to the average $\langle R(\mathcal{S}; \mathbf{x}) \rangle$ of the total number of aftershocks falling inside the area \mathcal{S} .

As can be seen from figures 3 and 4, it follows from (61) and from the properties of Mittag-Leffler functions that, if the large time window approximation (51) holds, one may use the approximate equality

$$\langle R(\tau, \mathcal{S}; \mathbf{x}) \rangle \simeq \langle R(\mathcal{S}; \mathbf{x}) \rangle. \quad (62)$$

In this large time window approximation, the relative rate (52) is transformed into

$$\mathcal{N}_{\text{in}}(\mathcal{S}) \simeq 1 - n + \frac{n(1 - n)}{2\pi^2 \ell^2} \int_0^{\infty} \frac{\tilde{\phi}(q)}{1 - n\phi(q)} \tilde{I}_{\mathcal{S}}^2(q) dq. \quad (63)$$

As the space domain \mathcal{S} increases in size, $\mathcal{N}_{\text{in}}(\mathcal{S})$ increases towards 1. Figure 5 plots $\mathcal{N}_{\text{in}}(\mathcal{S})$ using the space propagator $\phi(\mathbf{x})$ given by (9) for different values of the exponent η .

V. LARGE TIME WINDOW APPROXIMATION

The analysis of the previous section gives us the possibility to explore the probabilistic properties of the number of events in given space-time windows, in the regime where the large time window

approximation (51) holds. If the time duration τ of the space-time window is sufficiently large, the previous section has shown that the statistical averages and the seismic rates become independent of τ . It seems reasonable to conjecture that the GPF $\Theta(z, \tau, \mathcal{S}; \mathbf{x})$ of the total number of aftershocks triggered by some earthquake source inside the space domain \mathcal{S} until time τ coincides approximately with the saturated GPF $\Theta(z, \mathcal{S}; \mathbf{x})$ of the total number of aftershocks triggered by some earthquake source inside the space domain \mathcal{S} . Within this approximation of large time windows, the effect of aftershocks triggered by earthquake sources occurring till the beginning t of the time window is negligible. Section VII below will explore in more details the applicability of this conjecture.

Within this large time window approximation, one may ignore the first term in the r.h.s. of Eq. (22) and replace $\Theta(z, t, \mathcal{S}; \mathbf{x})$ by $\Theta(z, \mathcal{S}; \mathbf{x})$ in the remaining terms. As a result, Eq. (22) takes the following approximate form

$$L(z, \tau, \mathcal{S}) \simeq \tau \iint_{-\infty}^{\infty} [1 - \Theta(z, \mathcal{S}; \mathbf{x})][1 - I_{\mathcal{S}}(\mathbf{x})] d\mathbf{x} + \tau \iint_{\mathcal{S}} [1 - z\Theta(z, \mathcal{S}; \mathbf{x})] d\mathbf{x}, \quad (64)$$

where $\Theta(z, \mathcal{S}; \mathbf{x})$ is the solution of Eq. (29) with (30) or, equivalently, is the solution of

$$\Theta = G [\Theta \otimes \phi - (1 - z)I_{\mathcal{S}}\Theta \otimes \phi]. \quad (65)$$

where the function G is defined in (17).

A. Factorization procedure

To find a reasonable approximate expression for the sought GPF $\Theta(z, \mathcal{S}; \mathbf{x})$, notice that if $\ell \gg d$ (or if n is close to 1) then the characteristic spatial scale associated with the GPF $\Theta(z, \mathcal{S}; \mathbf{x})$ becomes greater than d . Therefore, without essential error, one may replace $\Theta \otimes \phi$ by Θ in (65). In addition, we take into account the finiteness of the domain \mathcal{S} by using the factorization procedure of replacing the last term of the argument of the function G in (65) as follows:

$$I_{\mathcal{S}}(\mathbf{x})\Theta(z, \mathcal{S}; \mathbf{x}) \otimes \phi(\mathbf{x}) \simeq \Theta(z, \mathcal{S}; \mathbf{x}) p_{\mathcal{S}}(\mathbf{x}), \quad (66)$$

where $p_{\mathcal{S}}(\mathbf{x})$ remains to be specified. We will show below that $p_{\mathcal{S}}(\mathbf{x})$ may be interpreted as the overall fraction of aftershocks, triggered by a mother earthquake at position \mathbf{x} , which fall within the domain \mathcal{S} . The factorization procedure amounts to replacing a convolution integral by an algebraic term. This factorization approximation is a crucial step of our analysis and will be justified further

below. As a result of its use, the nonlinear integral equation (65) transforms into the functional equation

$$\Theta = G[(1 + (z - 1)p_S(\mathbf{x}))\Theta]. \quad (67)$$

It is easy to show that, if relation (67) holds, then the average of the number of aftershocks corresponding to it is equal to

$$\langle R \rangle = \frac{n}{1 - n} p_S. \quad (68)$$

In the next subsection, we shall clarify what is the probabilistic sense of the parameter p_S . Here, it is sufficient to remark that one can determine it from a consistency condition: choose $p_S(\mathbf{x})$ such that the r.h.s. of Eq. (68) is equal to the true $\langle R(\mathcal{S}; \mathbf{x}) \rangle$. This gives

$$p_S(\mathbf{x}) = \frac{1 - n}{n} \langle R(\mathcal{S}; \mathbf{x}) \rangle, \quad \tilde{p}_S(\mathbf{q}) = \tilde{I}_S(\mathbf{q}) \tilde{\phi}(\mathbf{q}) \frac{1 - n}{1 - n \tilde{\phi}(\mathbf{q})}. \quad (69)$$

Figure 6 plots $p_S(\mathbf{x})$ defined by expression (69) as a function of dimensionless distance x/ℓ .

One can observe that, for $\ell \gg d$, the factor $p_S(\mathbf{x})$ approaches a rectangular function. We can use this observation to help determine the statistics of the number of events in a finite space-time window, using the approximation $p_S(\mathbf{x}) \simeq \text{const} = p$ for $\mathbf{x} \in \mathcal{S}$. We define the parameter p as the space average of $p_S(\mathbf{x})$ over the window's area \mathcal{S} :

$$p \simeq \frac{1}{S} \iint_{\mathcal{S}} p_S(\mathbf{x}) d\mathbf{x}. \quad (70)$$

p is thus the average over all possible spatial positions of mother earthquakes of the fraction of aftershocks which fall within the space-time window \mathcal{S} . The approximation $p_S(\mathbf{x}) \simeq \text{const} = p$ for $\mathbf{x} \in \mathcal{S}$ allows us to simplify the last term of (64) as follows:

$$\tau \iint_{\mathcal{S}} [1 - z\Theta(z, \mathcal{S}; \mathbf{x})] d\mathbf{x} \simeq \tau S [1 - z\Theta(z; p)], \quad (71)$$

where $\Theta(z, p)$ is the solution of

$$\Theta(z; p) = G[(1 + (z - 1)p)\Theta(z; p)], \quad (72)$$

which is derived from equation (67).

Complementarily, as can be seen from figure 6, $p_S(\mathbf{x})$ is small outside the window space domain \mathcal{S} . It implies that, outside \mathcal{S} , one may replace Eq. (67) by its linearized version. As a result, we get

$$1 - \Theta(z, \mathcal{S}; \mathbf{x}) \simeq \frac{n}{1 - n} (1 - z) p_S(\mathbf{x}). \quad (73)$$

Therefore, the first term in the r.h.s. of Eq. (64) transforms into

$$\tau \iint_{-\infty}^{\infty} [1 - \Theta(z, \mathcal{S}; \mathbf{x})][1 - I_{\mathcal{S}}(\mathbf{x})] d\mathbf{x} \simeq q\tau S \frac{n}{1-n}(1-z) , \quad (74)$$

where

$$q = \frac{1}{S} \iint_{-\infty}^{\infty} p_{\mathcal{S}}(\mathbf{x})[1 - I_{\mathcal{S}}(\mathbf{x})] d\mathbf{x} . \quad (75)$$

Taking into account that, due to (69),

$$\iint_{-\infty}^{\infty} p_{\mathcal{S}}(\mathbf{x}) d\mathbf{x} = S , \quad (76)$$

we obtain

$$q \simeq 1 - p . \quad (77)$$

Putting all these approximations together allows us to rewrite Eq. (64) in the form

$$L(z, \tau, \mathcal{S}) \simeq \tau S \left[\frac{n}{1-n}(1-p)(1-z) + 1 - z\Theta(z; p) \right] . \quad (78)$$

In what follows, we shall select a value of the parameter p which takes into account the finiteness of the window's spatial domain \mathcal{S} , to better fit empirical data on the statistics of seismic rates in finite space-time bins.

B. Probabilistic meaning of the factorization approximation (66) leading to (67) and (69)

The factorization approximation (66) has the following implication. Calling $\Theta(z)$ the GPF of the total number of aftershocks triggered over the whole space by some earthquake source, one can then determine the corresponding GPF $\Theta(z, \mathcal{S}; \mathbf{x})$ taking into account the finiteness of the space domain \mathcal{S} by using the relation

$$\Theta(z, \mathcal{S}; \mathbf{x}) = \Theta(q_{\mathcal{S}} + zp_{\mathcal{S}}) , \quad q_{\mathcal{S}}(\mathbf{x}) = 1 - p_{\mathcal{S}}(\mathbf{x}) . \quad (79)$$

This expression (79) has the following interpretation. Let the above mentioned earthquake source triggers r aftershocks. Then, the number of those aftershocks which fall into the space domain \mathcal{S} , is equal to

$$R_m(\mathcal{S}; \mathbf{x}|r) = X_1 + X_2 + \cdots + X_r , \quad (80)$$

where $\{X_1, \dots, X_r\}$ are mutually independent random variables equal to 1 with probability p_S and 0 with probability $q_S = 1 - p_S$. Thus, p_S is the fraction of the aftershocks which fall into the domain \mathcal{S} .

The corresponding expression (79) can be interpreted as follows. It gives the exact solution for the GPF of some specific space-time branching process, such that the pdf $f(\mathbf{y}; \mathbf{x})$ of the space positions \mathbf{y} of each aftershock is the same for all aftershocks and depends only on the position \mathbf{x} of the earthquake source. For this problem, we have

$$p_S(\mathbf{x}) = \iint_{-\infty}^{\infty} f(\mathbf{y}; \mathbf{x}) I_S(\mathbf{y}) d\mathbf{y}. \quad (81)$$

In the general case, the relation (79) offers the possibility, at least semi-quantitatively, to describe the characteristic features of the space-time branching processes, by using the probability p_S as an effective independent parameter of the theory.

Let us mention a few useful consequences of the relation (79). It implies that the probability that r aftershocks fall into the spatial domain \mathcal{S} is equal to

$$P(r, \mathcal{S}; \mathbf{x}) = \sum_{k=r}^{\infty} P(k) B(k, r, \mathcal{S}; \mathbf{x}), \quad (82)$$

where $P(k)$ is the probability that some earthquake source triggers k aftershocks and

$$B(k, r, \mathcal{S}; \mathbf{x}) = \binom{k}{r} p_S^r q_S^{k-r}. \quad (83)$$

This binomial probability $B(k, r, \mathcal{S}; \mathbf{x})$ is nothing but the conditional probability that, if the mother earthquake triggers $k \geq r$ aftershocks then, r of them will fall into the spatial domain \mathcal{S} . If $r \gg 1$, expression (83) can be approximated by its well-known Gaussian asymptotics

$$B(k, r, \mathcal{S}; \mathbf{x}) = \frac{1}{\sqrt{2\pi k p_S q_S}} \exp \left[-\frac{(r - k p_S)^2}{2k p_S q_S} \right]. \quad (84)$$

If, in addition, $P(k)$ decays slowly, for instance if it has a power asymptotic for $k \rightarrow \infty$, then expressions (82) and (84) imply the asymptotic relation

$$P(r, \mathcal{S}; \mathbf{x}) \sim \frac{1}{p_S} P\left(\frac{r}{p_S}\right) \quad (r \rightarrow \infty). \quad (85)$$

In view of this last relation (85), it seems reasonable to assume that the asymptotic behavior of the probabilities of the number of events for $r \gg 1$ are the same for the case of a finite \mathcal{S} ($p_S < 1$) and for an unbounded one ($p_S = 1$).

C. Large space-time windows

In order to get more insight into the properties of the statistics of seismic rates in finite space-time windows, it is useful to study the statistics of seismic rates in the limit where the space and time windows are large. In this case, \mathcal{N}_{in} in (63) and p in (70) are both close to 1 and one may replace Eq. (78) by

$$L(z, \tau, \mathcal{S}) \simeq \tau S [1 - z\Theta(z)], \quad (86)$$

where $\Theta(z)$ is solution of the functional equation

$$\Theta(z) = G[z\Theta(z)]. \quad (87)$$

Accordingly, the GPF of the number of events in a (large) space-time window as given by (31) takes the form

$$\Theta_{\text{sp}}(z, \rho) = \hat{f}(\rho [1 - z\Theta(z)]). \quad (88)$$

Here and everywhere below,

$$\rho = \langle \varrho \rangle \tau S. \quad (89)$$

Knowing the GPF $\Theta_{\text{sp}}(z, \tau; \mathcal{S})$, the probability $P_{\text{sp}}(r; \rho)$ of event numbers r is obtained from the formula

$$P_{\text{sp}}(r; \rho) = \frac{1}{r!} \left. \frac{\partial^r \hat{f}(\rho [1 - z\Theta(z)])}{\partial z^r} \right|_{z=0}. \quad (90)$$

Equivalently, the integral representation of (90) reads

$$P_{\text{sp}}(r; \rho) = \frac{1}{2\pi i} \oint_{\mathcal{C}} \hat{f}(\rho [1 - z\Theta(z)]) \frac{dz}{z^{r+1}}, \quad (91)$$

where \mathcal{C} is a sufficiently small contour in the complex plane z around the origin $z = 0$.

The main difficulty in calculating $P_{\text{sp}}(r; \rho)$ comes from the fact that the GPF $\Theta(z)$ is defined only implicitly by Eq. (87). To overcome this difficulty, we rewrite the integral in (91) in the following equivalent form

$$P_{\text{sp}}(r; \rho) = \frac{1}{2\pi i r} \oint_{\mathcal{C}} \frac{d\hat{f}(\rho [1 - z\Theta(z)])}{z^r} \quad (r > 0) \quad (92)$$

and use the new integration variable $y = z\Theta(z)$. Expression (87) shows that the inverse function of y is $z = y/G(y)$. As a result, the equation (92) transforms into

$$P_{\text{sp}}(r; \rho) = \frac{\rho}{2\pi i r} \oint_{\mathcal{C}'} G^r(y) Q(y; \rho) \frac{dy}{y^r}, \quad (93)$$

where

$$Q(z; \rho) = \frac{1}{\rho} \frac{d\hat{f}[\rho(1-z)]}{dz} \quad (94)$$

and \mathcal{C}' is a contour enveloping the origin $y = 0$ in the complex plane y . One may interpret $Q(z; \rho)$ (94) as the GPF of some random integer R_ρ such that $\langle R_\rho \rangle = \rho$.

Notice that Eq. (93) has a simple probabilistic interpretation. Indeed, it follows from (93) that

$$P_{\text{sp}}(r; \rho) = \frac{\rho}{r} \Pr \{R_\rho + R(r) = r - 1\}, \quad (95)$$

where R_ρ is a random integer with GPF $Q(z; \rho)$ given by (94) while

$$R(r) = R_1 + R_2 + \dots + R_r, \quad (96)$$

where $\{R_1, R_2, \dots, R_r, \dots\}$ are mutually independent random integers with GPF $G(z)$. This implies that the probabilities of each such random variable R_i , $i = 1, \dots, r$, has the power law asymptotics (19).

This remark provides a simple analysis of the asymptotic behavior of the probabilities $P_{\text{sp}}(r; \rho)$ for $r \gg 1$, by using expression (95). For $1 < \gamma < 2$, the asymptotics of the probability $P(k; r)$ that the sum (96) is equal to k goes to, for large r ,

$$P(k|r) \simeq \frac{1}{(\epsilon r)^{1/\gamma}} \psi_\gamma \left(\frac{k - nr}{(\epsilon r)^{1/\gamma}} \right), \quad (97)$$

where

$$\epsilon = - \left(n \frac{\gamma - 1}{\gamma} \right)^\gamma \Gamma(1 - \gamma) \quad (98)$$

and $\psi_\gamma(x)$ is the stable Lévy distribution with the two-sides Laplace transform

$$\int_{-\infty}^{\infty} \psi_\delta(x) e^{-sx} dx = e^{s^\delta}. \quad (99)$$

It is known that

$$\psi_\delta(x) \sim \frac{x^{-\delta-1}}{\Gamma(-\delta)} \quad (x \rightarrow \infty), \quad \psi_\delta(0) = \frac{1}{\delta \Gamma(1 - \frac{1}{\delta})}. \quad (100)$$

One can calculate $\psi_\delta(x)$ for any $1 < \delta < 2$, using, for instance, the following integral representation

$$\psi_\delta(x) = \frac{1}{\pi} \int_0^\infty \exp \left[-u^\delta + ux \cos \left(\frac{\pi}{\delta} \right) \right] \sin \left[ux \sin \left(\frac{\pi}{\delta} \right) + \frac{\pi}{\delta} \right] du. \quad (101)$$

For some numerical illustrations, we will use the case $\delta = 3/2$ for which the following analytical expression is available

$$\psi_{3/2}(x) = \frac{1}{\pi\sqrt{3}} \left[\Gamma\left(\frac{2}{3}\right) {}_1F_1\left(\frac{5}{6}, \frac{2}{3}, \frac{4x^3}{27}\right) - x \Gamma\left(\frac{4}{3}\right) {}_1F_1\left(\frac{7}{6}, \frac{4}{3}, \frac{4x^3}{27}\right) \right]. \quad (102)$$

For $r \gg \rho$, one can neglect the random integer R_ρ in the r.h.s. of Eq. (95) and obtain from (95) and (97) the following asymptotic formula

$$P_{\text{sp}}(r; \rho) \simeq \frac{\rho}{r(\epsilon r)^{1/\gamma}} \psi_\gamma \left(\frac{(1-n)r-1}{(\epsilon r)^{1/\gamma}} \right) \quad (r \gg \rho). \quad (103)$$

If $1-n \ll 1$ (the branching is close to but not exactly critical), Eq. (103) predicts the existence of two characteristic power laws in the dependence of the probabilities $P_{\text{sp}}(r; \rho)$ with r , a result already derived in [18].

1. For

$$1 \ll r \ll r_*, \quad \text{with } r_* = \left(\frac{1}{1-n} \right)^{\gamma/(\gamma-1)} \epsilon^{1/(\gamma-1)} \quad (104)$$

then,

$$P_{\text{sp}}(r; \rho) \sim r^{-1-1/\gamma}. \quad (105)$$

2. For

$$r \gg r_*, \quad (106)$$

we recover the original power law (19) of the number of first generation aftershocks

$$P_{\text{sp}}(r; \rho) \sim r^{-1-\gamma}. \quad (107)$$

For values of the parameters $\gamma = b/\alpha$ and n which are typical of real seismicity modeled by aftershock triggering processes, the cross-over number r_* separating the two power laws can be very large. For instance, for $\gamma = 1.25$ and $n = 0.9$, we obtain $r_* \simeq 10^4$.

D. Prediction of the distribution of event numbers for large time windows

Starting from the general expression (31) of the GPF $\Theta_{\text{sp}}(z, \tau; \mathcal{S})$ with the approximation (78) for $L(z, \tau, \mathcal{S})$ and using the relationship between the probability $P_{\text{sp}}(r; \rho, p)$ and its GPF similar to

expression (90) and its integral representation similar to (91), we obtain the following expression valid in the limit of large time windows

$$P_{\text{sp}}(r; \rho, p) = \frac{1}{2\pi i} \oint_{\mathcal{C}} \hat{f} \left(\rho \left[\frac{n}{1-n} (1-p)(1-z) + 1 - z\Theta(z; p) \right] \right) \frac{dz}{z^{r+1}} \quad (108)$$

where $\Theta(z; p)$ is the solution of the functional equation (72). Similarly to the change of variable used to go from (92) to (93), we introduce the new integration variable

$$y = (1 + (z-1)p)\Theta(z; p) \quad \Longleftrightarrow \quad z = Z(y) = \frac{1}{p} \left(\frac{y}{G(y)} + p - 1 \right). \quad (109)$$

By construction of y , $\Theta(z; p) = G(y)$ which allows us to obtain the following explicit expression

$$P_{\text{sp}}(r; \rho, p) = \frac{1}{2\pi i} \times \oint_{\mathcal{C}'} \hat{f} \left(\rho \left[\frac{n}{1-n} (1-p)(1-Z(y)) + 1 - Z(y)G(y) \right] \right) \frac{dZ(y)}{dy} \frac{dy}{Z^{r+1}(y)}. \quad (110)$$

This expression (110) allows us to make a precise quantitative prediction for the dependence of the distribution $P_{\text{sp}}(r; \rho, p)$ of the number r of earthquakes per space-time window as a function of r , once the model parameters n, γ, p, δ and ρ are given. We note that Pisarenko and Golubeva have shown that the distribution of numbers has the same tail as the distribution of seismic rates [9]. Thus, for the tails, our results can be interpreted either as statements on the distribution of realized numbers of earthquakes or on the distribution of average seismic rates.

We now turn to a brief description of the data analysis and of their fits with (110).

VI. EMPIRICAL ANALYSIS AND COMPARISON WITH THEORY

We use the Southern Californian earthquakes catalog with revised magnitudes (available from the Southern California Earthquake Center) as it is among the best one in terms of quality and time span. Magnitudes M_L are given with a resolution of 0.1 from 1932 to 2003, in a region from approximately 32° to 37°N in latitude, and from -114° to -122° in longitude. In order to maximize the size and quality of the data used for the analysis (to improve the statistical significance), we consider the sub-catalog spanning the time interval 1994 – 2003 for $M_L > 1.5$, which contains a total of 86,228 earthquakes. The completeness of this sub-catalog has been verified in the standard way in [29] by computing the complementary cumulative magnitude distribution for each year from

1994 to 2003 included. The stability of the linear relationship of the logarithm of the number as a function of magnitude M_L for $M_L > 1.5$ is taken as a diagnostic of completeness.

The spatial domain are covered by square boxes of $(L = 5 \text{ km}) \times (L = 5 \text{ km})$, which gives us 16046 spatial bins, with many of them being actually empty. This size is a compromise between conflicting requirements. On the one hand, a smaller spatial resolution should not be used due to the errors of localization of earthquake epicenters, which are of this order. On the other hand, increasing L decreases very fast ($\sim 1/L^2$) the total number of boxes with which the distribution of the number of events can be constructed. Four different sizes for the time window are considered: $dt = 1$ day (3652 temporal bins), $dt = 10$ days, $dt = 100$ days and $dt = 1000$ days. Combining the space and time windows leads to space-time windows or bins of size $L^2 \times dt$. For instance, for $dt = 1$ day, there is a total of 54669 spatio-temporal bins with at least one event, with 4298 non-empty spatial bins.

Figures 7-10 plot the empirical probability density functions $P_{\text{data}}(r)$ of the number r of earthquakes in the space-time bins described above. The straight line in Figs. 8-10 is the best fit with a pure power law

$$P_{\text{data}}(r) \sim 1/r^{1+\mu} \quad (111)$$

over the range $10 \leq r \leq 100$. The estimation for μ is found stable across different time windows, since the fitted values are $\mu = 1.65$ for $dt = 100$ days, $\mu = 1.75$ for $dt = 10$ days and $\mu = 1.60$ for $dt = 1$ days. However, one can also observe at the same time that the pdf becomes more and more curved in the larger portion of the bulk as the size dt of the time window is increased. This behavior can be explained by our theory as we know describe.

First, all parameters are let free to adjust optimally. The parameters are the branching ratio n defined by (6), the exponent γ defined in (5), the exponent δ defined in (15), the parameter $p_{\mathcal{S}} \simeq p$ coming from the factorization procedure (66) and given by (69) and (70) (which is roughly equal to the overall fraction of aftershocks triggered by sources in the domain \mathcal{S} which fall within the same domain \mathcal{S}), and the average number ρ of spontaneous earthquake source per space-time bin defined in (89). The theoretical curves shown in Figures 7-10 are obtained by a numerical integration of (110) for the set of parameters $n = 0.96$, $\gamma = 1.1$, $p = 0.25$, $\delta = 0.15$ and $\rho = 0.0019$ dt days with dt in units of days (thus equal to 1000 for Fig.7). Note that a given ρ for a given space-time window $[t, t + \tau] \times \mathcal{S}$ translates into the following average number of events inside that window:

$\langle R_{\text{sp}}(\tau, \mathcal{S}) \rangle \simeq \frac{\rho}{1-n} \simeq 0.02 - 0.16 \times dt$ (in units of days), taking the mean value $n = 0.96$. These parameters are chosen to best fit the empirical pdf for the largest time window $dt = 1000$ days shown in Fig. 7. They are then frozen and the theoretical distribution is recalculated with formula (110) with no adjustable parameters for the three other cases $dt = 100$ days (Fig. 8), $dt = 10$ days (Fig. 9) and $dt = 1$ day (Fig. 10). The theory is thus able to account simultaneously for all the considered time windows, with no adjustable parameters for the three smallest time windows.

Second, we test for the sensibility of the parameters. We actually obtain practically the same quality of fits for all four values $dt = 1, \dots, 1000$ days by varying δ and γ in the ranges $0.1 \leq \delta < 0.2$ and $1 \leq \gamma \leq 1.5$, by properly adjusting the other parameters adaptively. We do not show the corresponding theoretical curves as they are essentially equally good to fit the data within the empirical noise. The choice δ close to zero is consistent with the choice of the Cauchy distribution as a proxy for the heterogeneity of the spatial distribution of spontaneous earthquake sources inferred for the stress field and deduced from previous theoretical [25, 26] and empirical analysis of earthquake sources [24]. The strong sensitivity of the fits with respect to the fractal structure of the spontaneous sources quantified by the exponent δ is a surprising but positive return of this work. We did not expect a priori that the distribution of seismic rates would teach so much about the heterogeneity of the seismic active regions. But there is a lack of sensibility with respect γ . Thus, the distribution of seismic rates cannot be used to constrain the productivity parameter α (through $\gamma = b/\alpha$) other than by confirming the range of previous estimations of its value: $\alpha \approx 1$ [30, 31], $0.5 \leq \alpha < 1$ [20, 32, 33]. The sensitivity of the fits with respect to the branching ratio n and to the overall fraction p of aftershocks which fall within the domain \mathcal{S} requires a special discussion which will be reported elsewhere.

We have also used functional forms for $f_\delta(x)$ other than (15) to describe the pre-existing heterogeneity of spontaneous earthquake sources, such as half-Gaussian, exponential as well as different variants of power laws. Overall, we find that we need $f_\delta(x)$ to have a power law tail close to the Cauchy distribution in order to get a reasonable fit for all four time windows. This shows that the ETAS model as well as any other model of this class of triggered seismicity need to be generalized to account for a pre-existing heterogeneity of the crust, which controls the occurrence of the spontaneous earthquake sources.

We would also like to stress that, according to our theory, the value of the exponent $\mu \approx 1.6$ used in (111) to fit the tails of the distributions shown in Figs. 8-10 is describing a cross-over rather

than a genuine asymptotic tail. Recall that the distribution of the total number of aftershocks has two power law regimes $\sim 1/r^{1+\frac{1}{\gamma}}$ for $r < r_* \simeq 1/(1-n)^{\gamma/(\gamma-1)}$ and $\sim 1/r^{1+\gamma}$ for $r > r_*$ [18]. The existence of this cross-over together with the concave shape of the distribution at small and intermediate values of r combine to create an effective power law with an apparent exponent $\mu \approx 1.6$ larger than the largest asymptotic exponent γ . We have verified this to be the case in synthetically generated distributions with genuine asymptotics exponent $\gamma = 1.25$ for instance, which could be well fitted by $\mu \approx 1.6$ over several decades. We note also that Pisarenko and Golubeva [9], with a different approach applied to much larger spatial box sizes in California, Japan and Pamir-Tien Shan, have reported an exponent $\mu < 1$ which could perhaps be associated with the intermediate asymptotics characterized by the exponent $1/\gamma < 1$, found in our analysis [18]. By using data collapse with varying spatial box sizes on a California catalog, Corral finds that the distribution of seismic rates exhibits a double power-law behavior with $\mu \approx 0$ for small rates and $\mu \approx 1.2$ for large rates [2]. The first regime might be associated with the non universal bulk part of the distribution found in our analysis. The second regime is perhaps compatible with the prediction for the asymptotic exponent $\mu = \gamma$.

VII. THEORETICAL TESTS OF THE THEORY USING STATISTICS CONDITIONED ON GENERATION NUMBER

In our theoretical development to obtain the prediction (110) that could be compared with empirical data, we have been obliged to make two approximations: (1) assuming that the duration τ of the time window $[t, t + \tau]$ is sufficiently large (i.e., the inequality (51) holds), we have replaced the GPF $\Theta(z, \tau, \mathcal{S}; \mathbf{x})$ by its asymptotics $\Theta(z, \mathcal{S}; \mathbf{x})$; (2) we have used a factorization procedure to take into account quantitatively the finiteness of the spatial window \mathcal{S} .

In this section, we attempt to clarify further the domain of application of these two approximations by testing them on other event statistics conditioned on fixed number of generations. Numerical calculations of the exact PDF are compared with the approximations.

A. Large spatial windows

Let us consider the statistics of aftershocks triggered over the whole space during the first k generations by some mother event. The corresponding GPF of the number of aftershocks triggered in the course of k generations is defined by the following iterative recurrence equation

$$\Theta_k(z) = G[z\Theta_{k-1}(z)], \quad \Theta_1(z) = G(z). \quad (112)$$

One can calculate the corresponding probabilities of aftershock numbers by using the Cauchy integral

$$P_k(r) = \frac{1}{2\pi} \oint_C \Theta_k(z) \frac{dz}{z^{r+1}}. \quad (113)$$

Furthermore, we can make use of the knowledge that, as $k \rightarrow \infty$, the GPF $\Theta_k(z)$ converges to the asymptotic GPF $\Theta(z)$ which is the solution of Eq. (87). It is easy to show that one can calculate the corresponding probabilities using an equality analogous to (93):

$$P(r) = \frac{1}{2\pi i(r+1)} \oint_{C'} G^{r+1}(y) \frac{dy}{y^{r+1}}. \quad (114)$$

Figure 11 shows the distribution $P_k(r)$ of aftershocks numbers, obtained by a numerical calculation of the integral (113) for different values $k = 1, 2, 3, 5, 8$ and for $\gamma = 1.25$ and in the critical case $n = 1$. It also shows the corresponding asymptotic distribution for $k \rightarrow +\infty$ obtained by integration of (114). Note that, even for in this critical case, the distribution for $k = 8$ generations is already almost undistinguishable from the asymptotic distribution including an infinite number of generations, at least for $r \leq 250$. Figure 12 clarifies further the convergence rate by plotting the ratio

$$p_k(r) = \frac{P_k(r)}{P(r)} \quad (115)$$

for different values k .

The information on the number of generations necessary to reach the asymptotic regime gives us the possibility of estimating the corresponding characteristic time beyond which the asymptotic distribution $P(r)$ becomes a good approximation of $P_k(r)$. Let $T(k)$ denote the random time at which a k -th generation aftershock is triggered. It is equal to

$$T(k) = \tau_1 + \tau_2 + \cdots + \tau_k, \quad (116)$$

where $\{\tau_1, \tau_2, \dots, \tau_k, \dots\}$ are mutually independent random waiting times between the occurrence of a mother earthquake and one of its first-generation aftershock. We define the ω -th waiting time quantile $t(\omega, k)$ of generation k by

$$\mathcal{Q}[t(\omega, k), k] = \Pr\{T(k) > t(\omega, k)\} = \omega. \quad (117)$$

Thus, $1 - \omega$ is the probability that the duration of any chain of k successive generations of triggered aftershocks is smaller than $t(\omega, k)$. Choosing some confidence level (for example $1 - \omega = 0.9$), one may assert that, during the time $t(\omega, k)$, all aftershocks of the k -th generation have already been triggered. Let $k = k_*$ be such that the corresponding probability $P_{k_*}(r)$ is close to the asymptotic $P(r)$. Then, one may interpret

$$t_* = t(\omega, k_*) \quad (118)$$

as an estimation of the characteristic time for the validity of the asymptotic distribution $P(r)$.

The asymptotic expression for the probability $\mathcal{Q}(t, k)$ defined by (117) for $k \gg 1$ can be determined by using the fact that the terms τ_k of the sum (116) are determined by Omori's law (8) with $0 < \theta < 1$. For $k \gg 1$, $\mathcal{Q}(t, k)$ is asymptotically close to

$$\mathcal{Q}(t, k) = F_\theta \left(\frac{t}{c[k\Gamma(1 - \theta)]^{1/\theta}} \right), \quad (119)$$

where

$$F_\theta(x) = \int_x^\infty \varphi_\theta(y) dy \quad (120)$$

and $\varphi_\theta(x)$ is the one-sided Lévy stable distribution defined by the Laplace transform

$$\hat{\varphi}_\theta(u) = \int_0^\infty \varphi_\theta(x) e^{-ux} dx = e^{-u^\theta}. \quad (121)$$

In particular

$$F_{1/2}(x) = \operatorname{erf} \left(\frac{1}{2\sqrt{x}} \right). \quad (122)$$

The following asymptotic behavior holds

$$F_\theta(x) \simeq \frac{x^{-\theta}}{\Gamma(1 - \theta)} \quad (x \gg 1). \quad (123)$$

Substituting (119) and (123) into (117), we obtain the following estimation for t^* defined by (118)

$$t_* \simeq c \left(\frac{k_*}{\omega} \right)^{1/\theta}. \quad (124)$$

For instance, for $\theta = 1/2$, $k_* = 8$, $\omega = 0.1$ and $c = 2$ minutes, then $t_* \simeq 9$ days. Note that t_* is highly sensitive to the value of θ . Indeed, $\theta = 1/3$ (resp. $2/3$) with all other parameters being the same gives $t_* \simeq 700$ days (resp. $t_* \simeq 1$ day).

Expression (124) is related to condition (51) (and actually improves on it) as follows. The condition (51) with (50) can be expressed by introducing, similarly to the reasoning leading to (124), some small threshold $\omega \ll 1$ such that (51) translates into $\mathcal{N}_{\text{out}}(\tau) \lesssim \omega$. Correspondingly, we can introduce τ^* such that, if $\tau > \tau^*$, then the duration of the window is large at the ω level:

$$\omega \simeq \frac{n}{\Gamma(1-\theta)} \left(\frac{c_1}{\tau^*} \right)^\theta. \quad (125)$$

Using (45), we get

$$\tau^* \simeq c \left(\frac{n}{\omega(1-n)} \right)^{1/\theta}. \quad (126)$$

The two expressions (126) and (124) have a similar structure. The only difference is that the characteristic generation number k_* is replaced by the factor $n/(1-n)$. For n not too close to 1, $n/(1-n)$ gives a not unreasonable estimation of k_* . For n close to 1, expression (124) should be preferred as it provides an improvement to (51) based on the calculation of quantiles rather than on the mean rate behavior.

B. Finite spatial windows

A natural generalization of the iterative procedure (112) for finite spatial window \mathcal{S} allows to estimate the corresponding aftershock statistics. Consider an earthquake occurring at point \mathbf{x} . Then, the pdf of the space positions \mathbf{y} of an aftershock of the k -th generation is given by $\phi_k(\mathbf{y} - \mathbf{x})$, where

$$\phi_k(\mathbf{y}) = \phi(\mathbf{y}) \underbrace{\otimes \cdots \otimes}_k \phi(\mathbf{y}) \quad (127)$$

is the k -times convolution of the space propagator $\phi(\mathbf{y})$ (one example is given by (9)). Correspondingly, the probability for an aftershock of the k -th generation to fall into the space window \mathcal{S} is equal to

$$p_k(\mathcal{S}; \mathbf{x}) = \iint_{\mathcal{S}} \phi_k(\mathbf{y} - \mathbf{x}) d\mathbf{y}. \quad (128)$$

Provided these probabilities are known, one can determine the GPF $\Theta_k(z, \mathcal{S}; \mathbf{x})$ of the number of aftershocks of the k generation occurring in the spatial domain \mathcal{S} by using the following iteration

$$\begin{aligned}\Theta_1(z, \mathcal{S}; \mathbf{x}) &= G(p_1(z-1) + 1) , \\ \Theta_2(z, \mathcal{S}; \mathbf{x}) &= G[(p_1(z-1) + 1) G(p_2(z-1) + 1)] , \\ \Theta_2(z, \mathcal{S}; \mathbf{x}) &= G[(p_1(z-1) + 1) G[(p_2(z-1) + 1) G[(p_3(z-1) + 1)]]] ,\end{aligned}\tag{129}$$

and so on up to the order k . Then, the distribution of the number of aftershocks of the k generation is given by

$$P_k(r, \mathcal{S}; \mathbf{x}) = \frac{1}{2\pi} \oint_{\mathcal{C}} \Theta_k(z, \mathcal{S}; \mathbf{x}) \frac{dz}{z^{r+1}} .\tag{130}$$

These expressions are general and hold for any space propagator $\phi(\mathbf{y})$. Let us now specialize to the form (9) for the spatial propagator $\phi(\mathbf{y})$, with $\eta = 1$,

$$\phi_k(\mathbf{x}) = \frac{kd}{2\pi(x^2 + k^2d^2)^{3/2}}\tag{131}$$

corresponding to an asymptotic $1/|\mathbf{x}|^3$ decay law often argued on the basis of the shape of the elastic Green function in a three dimensional space. From (128), we then have

$$p_k(\mathcal{S}; \mathbf{x}) = \mathcal{P}\left(\frac{\ell}{kd}, \frac{x}{kd}\right)\tag{132}$$

where

$$\mathcal{P}(u, v) = \frac{2}{\pi} \int_0^u E\left(\frac{4vs}{1 + (v+s)^2}\right) \frac{sds}{[1 + (v-s)^2]\sqrt{1 + (v+s)^2}} .\tag{133}$$

Here, $E(m)$ is the complete elliptic integral

$$E(m) = \int_0^{\pi/2} \sqrt{1 - m \sin^2 \epsilon} d\epsilon .\tag{134}$$

Figure 13 shows the distributions (132) for $\ell = 10d$ (recall that ℓ is the radius of the assumed circular domain \mathcal{S} centered on the origin, which has been used in (58)) and for different positions \mathbf{x} of the mother earthquake, given by $x/\ell = 0; 0.4; 0.6; 0.8; 1; 1.2; 1.4; 1.6$ from top to bottom. The separation by the curve for $x/\ell = 1$ into two families has a simple explanation. For $x/\ell \leq 1$, the mother event lies within the spatial domain \mathcal{S} of interest and it is thus counted as generation 0. Its immediate aftershocks are most probably adjacent to it and thus have a large probability to also fall within \mathcal{S} . As the number k of generation increases, aftershocks diffuse away and are less and less likely to fall within \mathcal{S} . In contrast, for $x/\ell > 1$, the mother earthquake falls outside

\mathcal{S} . Therefore, there is not event at the zeroth generation in \mathcal{S} , hence the curves start from zero. The first generations of aftershocks which are most likely to be nearby the mother earthquake fall rarely within \mathcal{S} . Only as aftershocks of higher generation levels develop and diffuse away from the mother earthquake, can they invade \mathcal{S} . Of course, at large generation numbers, the aftershocks diffuse away from any finite spatial domain, explaining the decay of $P_k(\mathcal{S}; \mathbf{x})$ to zero for large k 's.

Figure 14 plots the asymptotic distribution $P(r, \mathcal{S}; \mathbf{x})$ as a function of the number r of aftershocks for $\gamma = 1.25$, $n = 0.99$, for different values of the radius ℓ of the disk \mathcal{S} . The mother earthquake is assumed to occur at the origin, that is, at the center of the disk \mathcal{S} . $P(r, \mathcal{S}; \mathbf{x})$ is obtained by using (130) for $k = 25$ generations, which is certainly a very good approximation to $P(r, \mathcal{S}; \mathbf{x}) = P_{k \rightarrow +\infty}(r, \mathcal{S}; \mathbf{x})$. Figure 15 plots $P(r, \mathcal{S}; \mathbf{x})$ as a function of the number r of aftershocks, at fixed $\ell/d = 10$ for various positions of the mother earthquake, for the same parameters $\gamma = 1.25$, $n = 0.99$. One can observe that, when the mother earthquake is inside the disk \mathcal{S} ($x = 0.8\ell; 0.6\ell; 0.4\ell; 0.2\ell; 0$), the corresponding distributions are close to each other as predicted in Section V A. When the mother is outside the disk \mathcal{S} ($x = 1.4\ell; 1.2\ell; 1$), the distributions differ from the previous case and are significantly smaller. This gives additional support in favor of the linear approximation (73), which we used in Section V A. More precisely, these properties result directly from the analysis of section V A, in which we notice below equation (69) that, for $\ell \gg d$, the factor $p_{\mathcal{S}}(\mathbf{x})$ approaches a rectangular function, which leads to the approximation $p_{\mathcal{S}}(\mathbf{x}) \simeq \text{const} = p$ for $\mathbf{x} \in \mathcal{S}$. This leads to the natural assumption that the GPF $\Theta(z, \mathcal{S}; \mathbf{x})$ is almost the same for all interior source positions $\mathbf{x} \in \mathcal{S}$. This means in turn that the corresponding distribution $P(r, \mathcal{S}; \mathbf{x})$ should be the same for all $\mathbf{x} \in \mathcal{S}$. This remarkable fact is illustrated in figure 15 in which the curves for the interior source probabilities merge.

C. Testing the factorization approach

We can now test the factorization approximation developed in section V A to take into account the finiteness of the space window \mathcal{S} by comparing it with the approach in term of the statistics over successive generations of the previous section. We thus compare the asymptotic distribution $P(r, \mathcal{S}, \mathbf{x} = 0)$, obtained by calculating the integral (130) for a large enough generation number k

($k = 25$ is found to be sufficient), with the factorization approximation

$$P(r, p) = \frac{p^r}{2\pi r} \oint_{\mathcal{C}'} \frac{dG(y)}{dy} \frac{G^r(y) dy}{[y - (1 - p)G(y)]^r}, \quad (135)$$

with an appropriate value of the parameter $p = p_S$, defined as the fraction of the aftershocks which fall into the domain \mathcal{S} . Figure 16 shows this comparison for four different values of $\ell/d = 10; 7.5; 5; 2.5$. The upper curve in each panel is the distribution (114) for an infinite domain $\ell/d = +\infty$, as a reference. There is some discrepancy between $P(r, \mathcal{S}, \mathbf{x} = 0)$ and $P(r, p)$ given by (135). The main difference is that the true distribution $P(r, \mathcal{S}, \mathbf{x} = 0)$ decays faster than the factorization approximation $P(r, p)$ for large r . We recall that, due to (85), the asymptotic behavior of the distribution $P(r, p)$ obtained under the factorization approximation is the same as for an infinite domain given by (114). Nevertheless, Figure 16 shows that an appropriate choice of the parameter $p = p_S$ allows us, at least semi-quantitatively, to take into account the finiteness of the area \mathcal{S} .

VIII. DISCUSSION

We have presented a general formulation in terms of generating functions of the space-time organization of earthquake sequences, in the framework of general branching processes. We have applied this approach to the ETAS (Epidemic-Type Aftershock Sequence) model of triggered seismicity. In view of the formidable difficulty in obtaining exact solutions to the nonlinear integral equations involving the generating functions, we have developed several approximation schemes which have been tested by comparison with exact numerical calculations. We have used the corresponding predictions to fit the distribution of seismic rates in four finite space-time windows in a California seismic catalog. The space-time windows differ by their time interval going from $dt = 1$ day to $dt = 1000$ days. The fits have been found to account satisfactorily for the empirical observation. In particular, we have adjusted the parameters of the theory on the largest time window $dt = 1000$ days and have then used these frozen parameter values in the theory to calculate the distribution for the smaller time windows. This tests the rigidity of the theory to account simultaneously for the distributions at different time scales. In this process, we have found it necessary to augment the ETAS model by taking account of the pre-existing frozen heterogeneity of spontaneous earthquake sources. We have discussed the physical justification of this generalization in terms of pre-existing

stress and fault networks, which constrain the form of the pre-existing heterogeneity. Our findings have also important implications to assess the quality of models developed to forecast future seismicity, and suggest to re-examine current procedures which assume Poisson statistics in the construction of likelihood scores.

Acknowledgments: We thank warmly G. Ouillon for help in the analysis of the data and in the preparation of the corresponding figures. This work is partially supported by NSF-EAR02-30429, and by the Southern California Earthquake Center (SCEC) SCEC is funded by NSF Cooperative Agreement EAR-0106924 and USGS Cooperative Agreement 02HQAG0008. The SCEC contribution number for this paper is xxx.

-
- [1] Bak, P., K. Christensen, L. Danon and T. Scanlon, *Phys. Rev. Lett.* 88, 178501 (2002).
 - [2] Corral A., *Physical Review E.* 6803(3 Part 2), 5102, 2003.
 - [3] M. S. Mega, P. Allegrini, P. Grigolini, V. Latora, L. Palatella, A. Rapisarda and S. Vinciguerra, *Phys. Rev. Lett.*, 90, 18850, 2003.
 - [4] Abe, S. and N. Suzuki, *Europhys. Lett.*, 65 (4), 581-586, 2004.
 - [5] Baiesi, M. and M. Paczuski, *Phys. Rev. E*, 69, 066106, 2004.
 - [6] Baiesi, M. and M. Paczuski, Complex networks of earthquakes and aftershocks, preprint at <http://arxiv.org/abs/physics/0408018>
 - [7] Baiesi, M. Scaling and precursor motifs in earthquake networks, preprint at <http://arxiv.org/abs/cond-mat/0406198>
 - [8] Schorlemmer, D., M. Gerstenberger, S. Wiemer, and D. Jackson, Earthquake likelihood model testing, preprint, 2004.
 - [9] V.F. Pisarenko and T.V. Golubeva, *Computational Seismology and Geodynamics*, 4, 127-137, 1996.
 - [10] Ogata, Y., *J. Am. Stat. Assoc.*, 83, 9-27, 1988.
 - [11] Kagan, Y.Y. and L. Knopoff, *J. Geophys. Res.*, 86, 2853 (1981).
 - [12] Helmstetter, A. and D. Sornette, earthquake aftershocks, *J. Geophys. Res.*, 107 (B10) 2237, doi:10.1029/2001JB001580 (2002).

- [13] Helmstetter, A. and D. Sornette, *J. Geophys. Res.*, *108 (B10)*, 2457 10.1029/2003JB002409 01, 2003.
- [14] Athreya, K.B. and P. Jagers, eds., *Classical and modern branching processes* (Springer, New York, 1997).
- [15] Sankaranarayanan, G., *Branching processes and its estimation theory* (Wiley, New York, 1989).
- [16] Helmstetter, A. and D. Sornette, *Physical Review E*, *6606*, 061104, 2002.
- [17] Helmstetter, A., G. Ouillon and D. Sornette, *J. Geophys. Res.*, *108*, 2483, 10.1029/2003JB002503, 2003.
- [18] Saichev, A., A. Helmstetter and D. Sornette, Anomalous Scaling of Offspring and Generation Numbers in Branching Processes, in press in *Pure and Applied Geophysics*, 2004 (<http://arXiv.org/abs/cond-mat/0305007>)
- [19] Saichev, A. and D. Sornette, Anomalous Power Law Distribution of Total Lifetimes of Aftershocks Sequences, in press in *Phys. Rev. E*, 2004. (<http://arXiv.org/abs/physics/0404019>)
- [20] Helmstetter, A., *Phys. Rev. Lett.*, *91*, 058501, 2003.
- [21] Sornette, D. and M.J. Werner, Constraints on the size of the smallest triggering earthquake from the ETAS Model, Båth's law, and observed aftershock sequences, *J. Geophys. Res.*, 2004 (<http://arxiv.org/abs/physics/0411114>).
- [22] Sornette, A. and D. Sornette, *Geophys. Res. Lett.*, *6*, 1981-1984, 1999.
- [23] Gorshkov, A., V. Kossobokov and A. Soloviev, Recognition of earthquake prone areas, in *Nonlinear dynamics of the lithosphere and earthquake prediction*, V. I. Keilis-Borok and A.A. Soloviev, eds. (Springer, Heidelberg) 239-310.
- [24] Kagan, Y.Y., *Nonlinear Processes in Geophysics*, *1*, 171-181, 1994.
- [25] Zolotarev, V. M. and Strunin, B.M., *Soviet Phys. Solid State*, *13*, 481-482, 1971.
- [26] Zolotarev, V. M., *One-dimensional Stable Distributions*, Amer. Math. Soc. Providence R.I., 1986.
- [27] Sornette, D., *Critical Phenomena in Natural Sciences*, Chaos, Fractals, Self-organization and Disorder: Concepts and Tools, 2nd ed. (Springer Series in Synergetics, Heidelberg, 2004).
- [28] Helmstetter, A. and D. Sornette, model of seismicity, *Geophys. Res. Lett.* *30* (11) doi:10.1029/2003GL017670, 2003.
- [29] Ouillon, G. and D. Sornette, Magnitude-Dependent Omori Law: Empirical Study and Theory, in press in *J. Geophys. Res.*, 2004 (<http://arXiv.org/abs/cond-mat/0407208>)

- [30] Felzer, K. R., T. W. Becker, R. E. Abercrombie, G. Ekstroem, and J. R. Rice *J. Geophys. Res.*, *107*(B9), 2190, doi:10.1029/2001JB000911, 2002.
- [31] Helmstetter, A., Y. Y. Kagan, and D. D. Jackson, Importance of small earthquakes for stress transfers and earthquake triggering, *J. Geophys. Res.*, submitted, 2004 (<http://xxx.lanl.gov/abs/physics/0407018>).
- [32] Console, R., M. Murru, and A. M. Lombardi, *J. Geophys. Res.*, *108*(B10), 2468, doi:10.1029/2002JB002123, 2002.
- [33] Zhuang, J., Y. Ogata, and D. Vere-Jones *J. Geophys. Res.* *109*, B05301, doi:10.1029/2003JB002879, 2004.
- [34] Gardner, J. K. and L. Knopoff, *Bull. Seismol. Soc. Amer.* *64*, 1363-1367, 1974.
- [35] Reasenber, P., *J. Geophys. Res.* *90*, 5479-5495, 1985.
- [36] Davis, S. D., and C. Frohlich, *J. Geophys. Res.*, *96*(B4), 6335-6350, 2001.

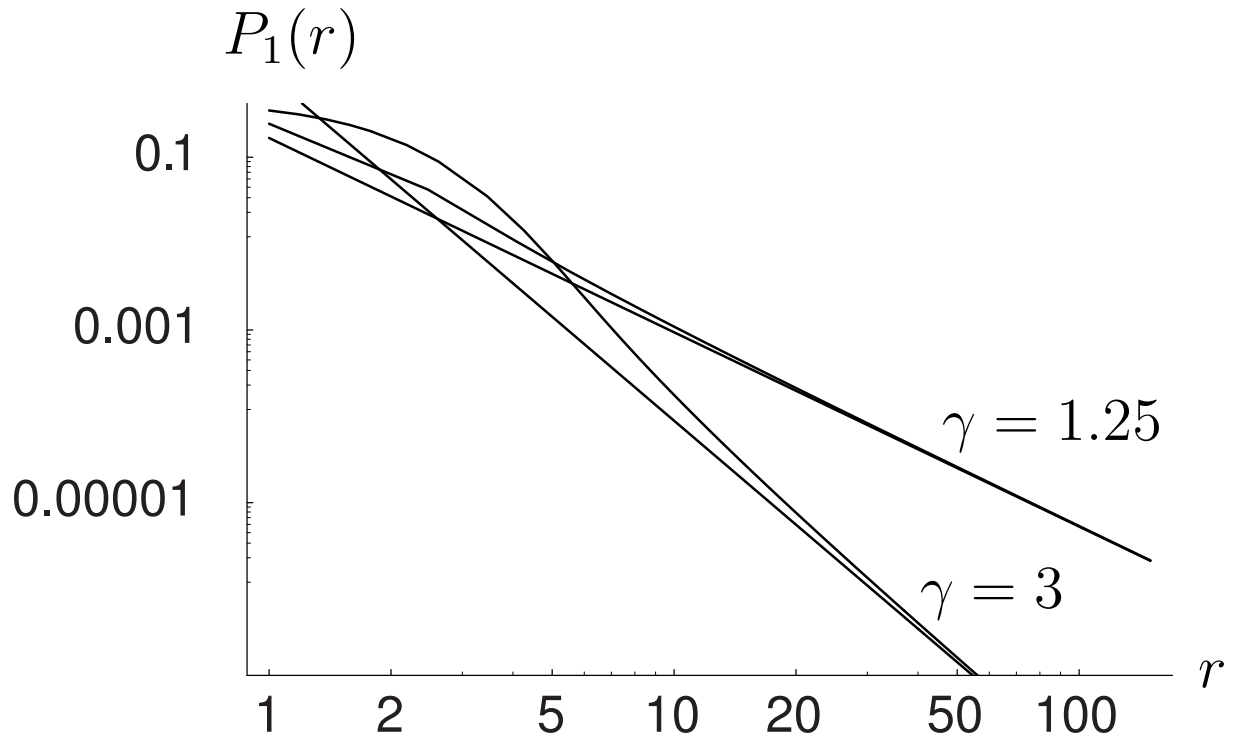


Fig. 1: Plot of the probabilities (18) and their power law asymptotics (19) for the infinite variance case $\gamma = 1.25$ and for a finite variance case $\gamma = 3$.

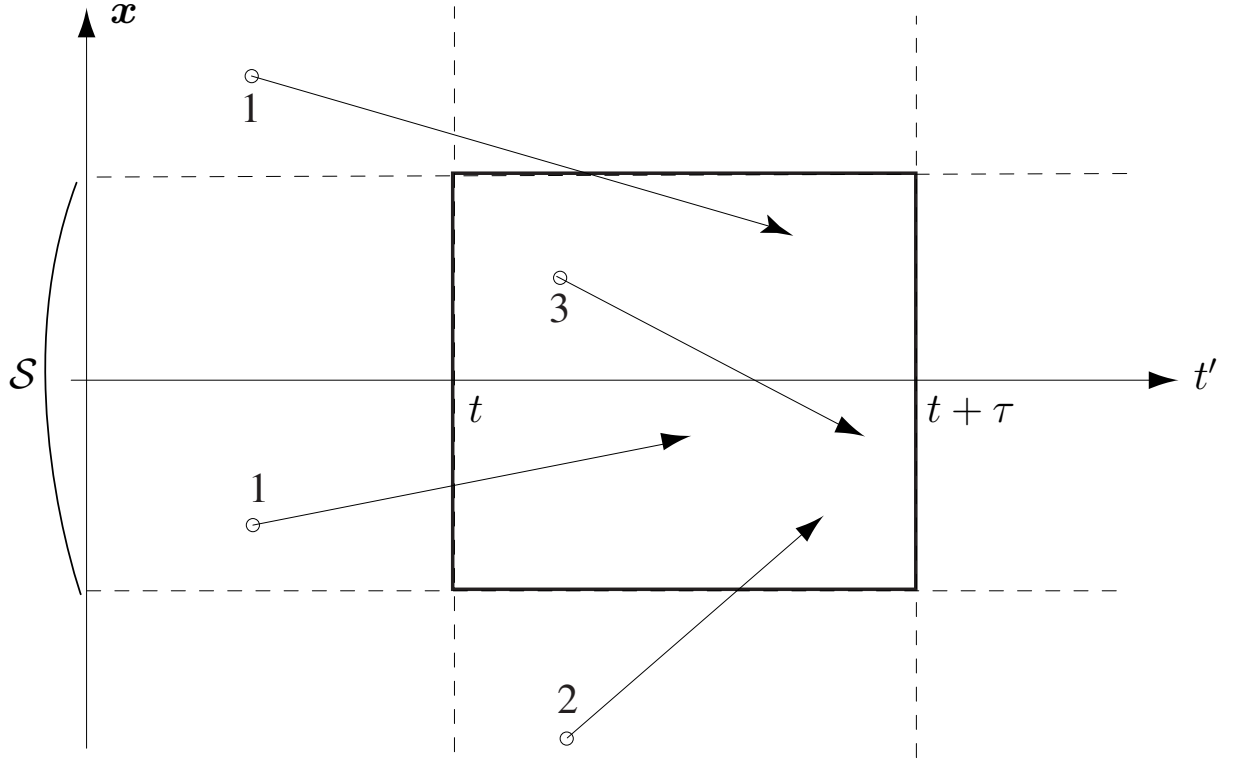


Fig. 2: Illustration of the three different sets of space-time locations for mother earthquakes contributing to the three terms in the r.h.s. of expression (22).

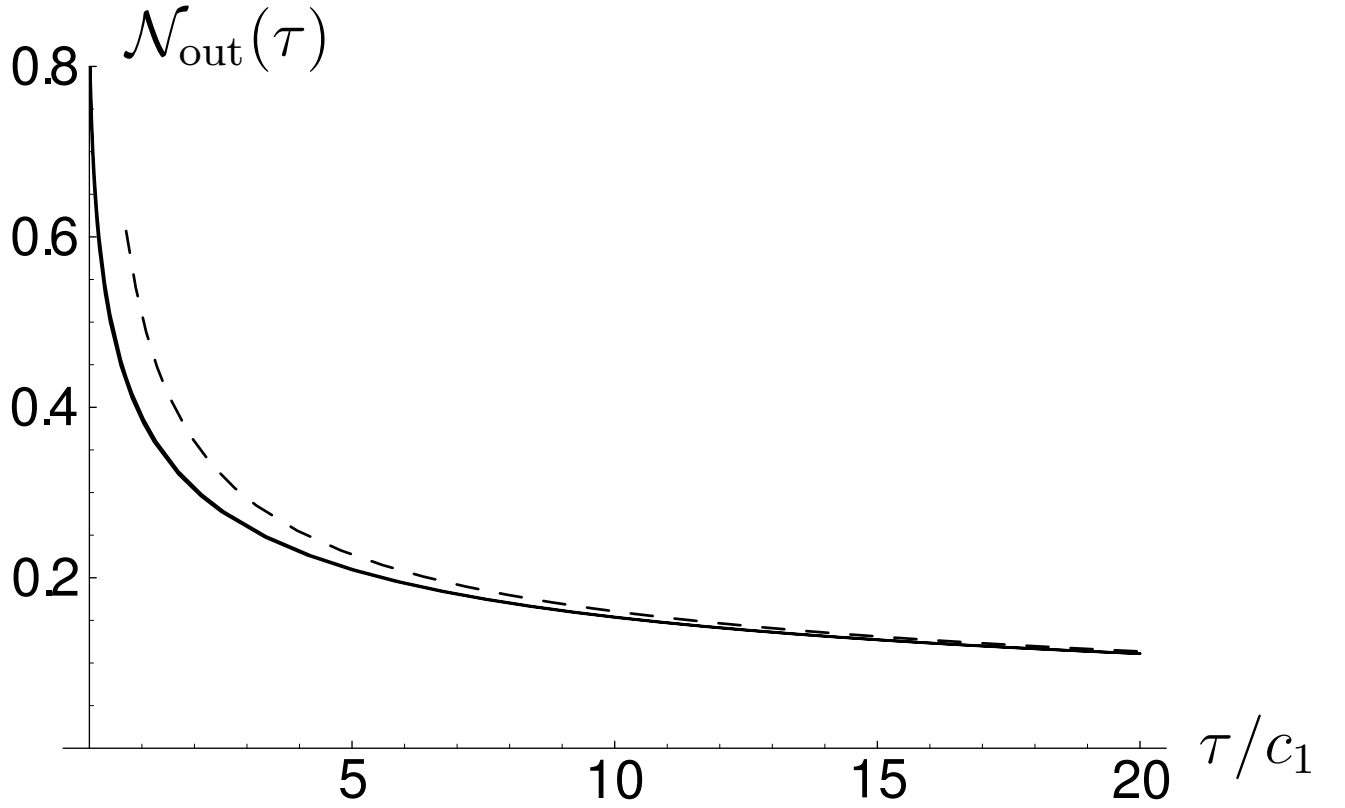


Fig. 3: Plots of the exact rate $\mathcal{N}_{\text{out}}(\tau)$, its fractional approximation (46) (which actually coincides with the exact value) and its asymptotic approximation (50) obtained from (48) (dashed line), for $n = 0.9$ and $\theta = 1/2$.

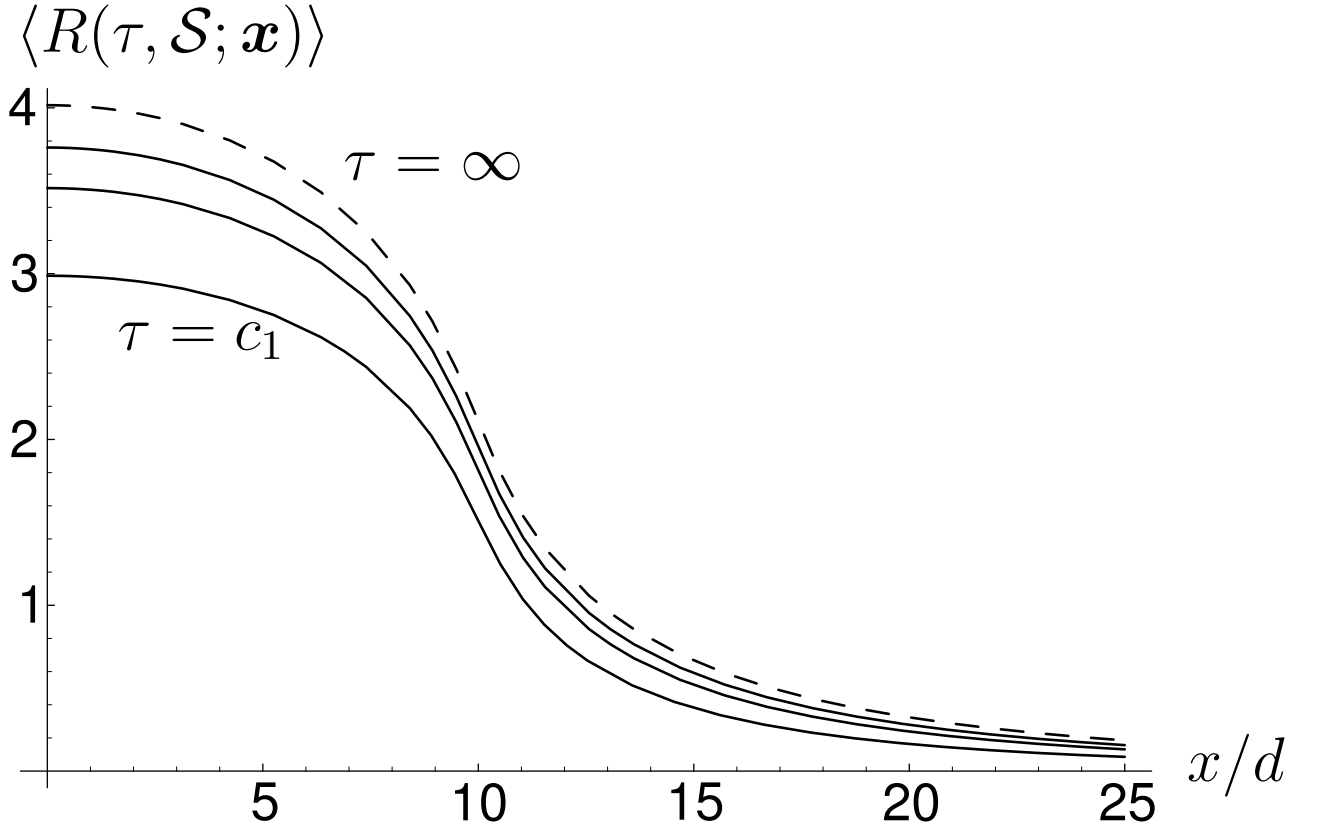


Fig. 4: Plots of $\langle R(\tau, \mathcal{S}; \mathbf{x}) \rangle$ for $\eta = 1$, $\ell = 10d$, $\theta = 1/2$ and for $\tau = c_1$; $5c_1$; $20c_1$. Dashed line is the plot of average of total number of aftershocks, falling into the circle \mathcal{S} .

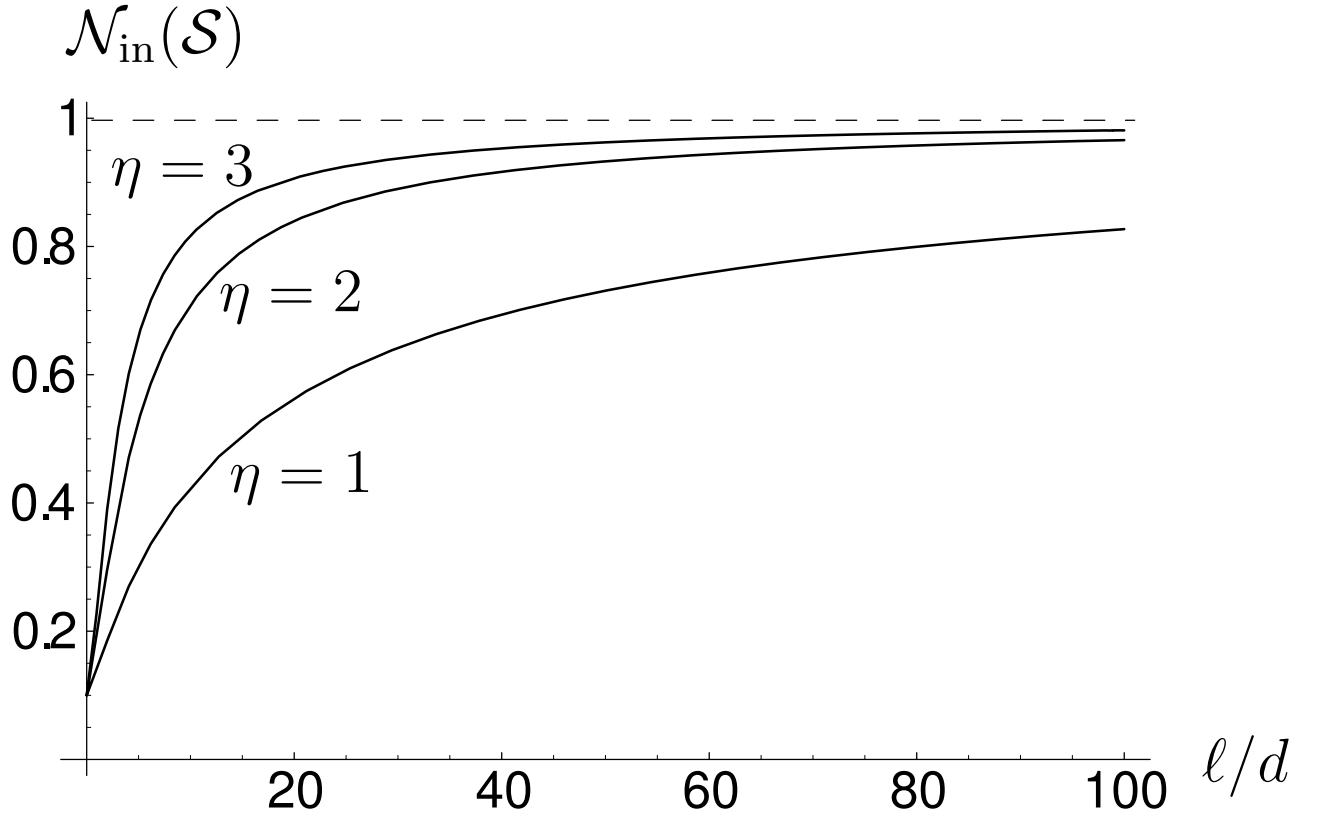


Fig. 5: Plots of the relative rate $\mathcal{N}_{\text{in}}(\mathcal{S})$ given by (63) as a function of the dimensionless size ℓ/d of the space domain, for different exponents $\eta = 1; 2; 3$ of the space propagator.

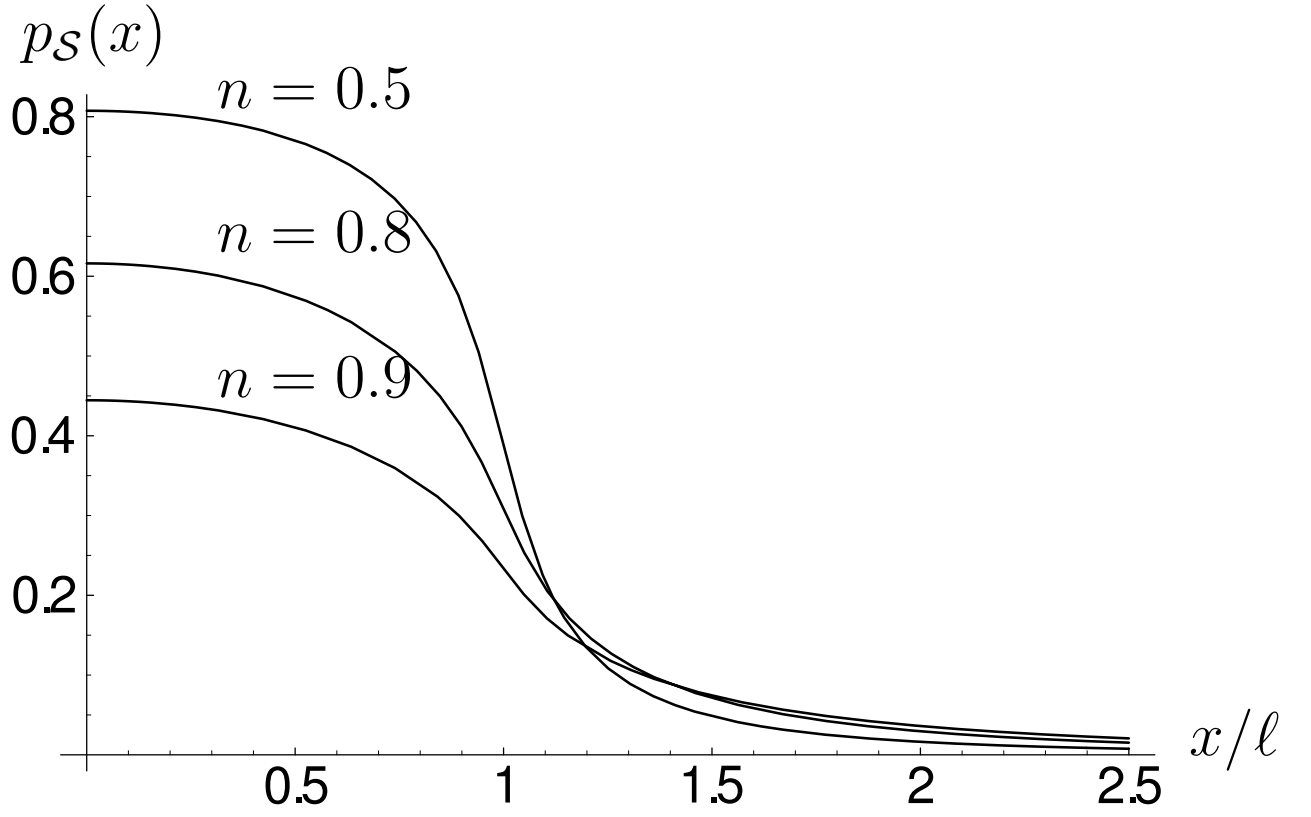


Fig. 6: Plots of the self-consistent factor $p_S(x)$ defined by (69) for $\ell = 10d$ and for $n = 0.5; 0.8; 0.9$.

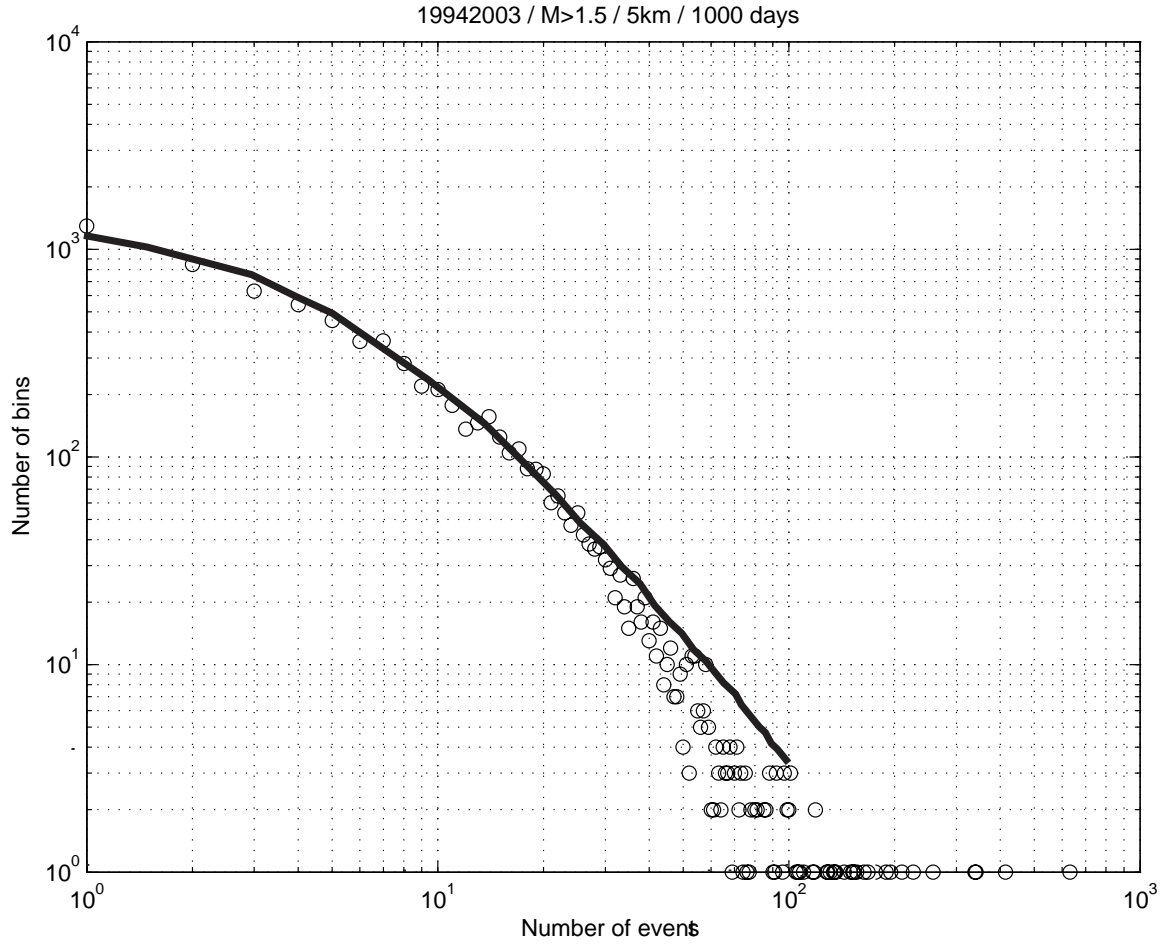


Fig. 7: Empirical probability density functions $P_{\text{data}}(r)$ of the number r of earthquakes in the space-time bins of size $5 \times 5 \text{ km}^2$ and $dt = 1000$ days. The continuous line is the fit of this data with formula (110) for the set of parameters $n = 0.96$, $\gamma = 1.1$, $p_S = 0.25$, $\delta = 0.15$ and $\rho = 0.0019 \text{ km} \times 1000 \text{ days}$.

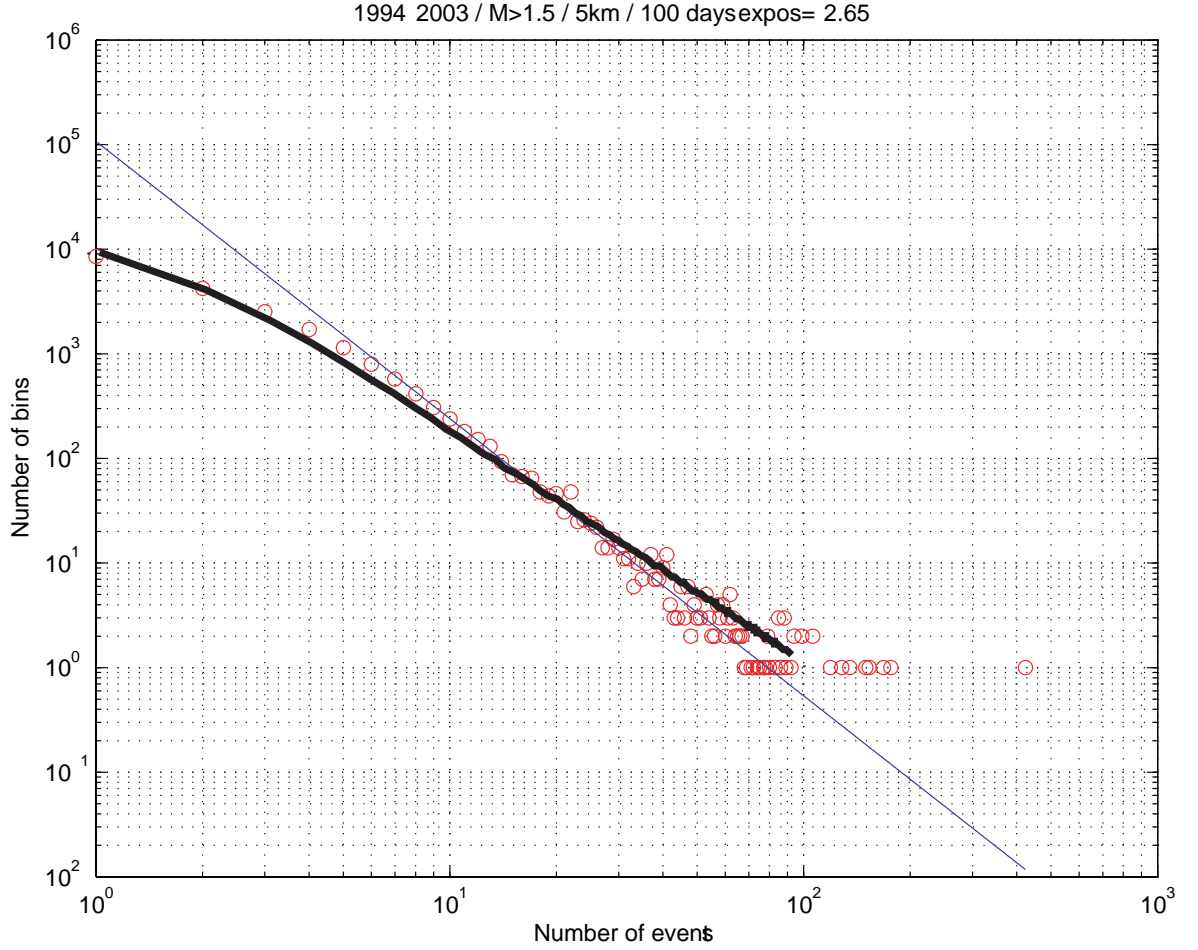


Fig. 8: Empirical probability density functions $P_{\text{data}}(r)$ of the number r of earthquakes in the space-time bins of size $5 \times 5 \text{ km}^2$ and $dt = 100$ days. The straight line is the best fit with a pure power law $P_{\text{data}}(r) \sim 1/r^{1+\mu}$ over the range $10 \leq r \leq 100$, which gives $\mu = 1.65$. The continuous line is the theoretical prediction using formula (110) with $dt = 100$ days and with no adjustable parameters, as the parameters are fixed to the values adjusted from the fit in Fig.7.

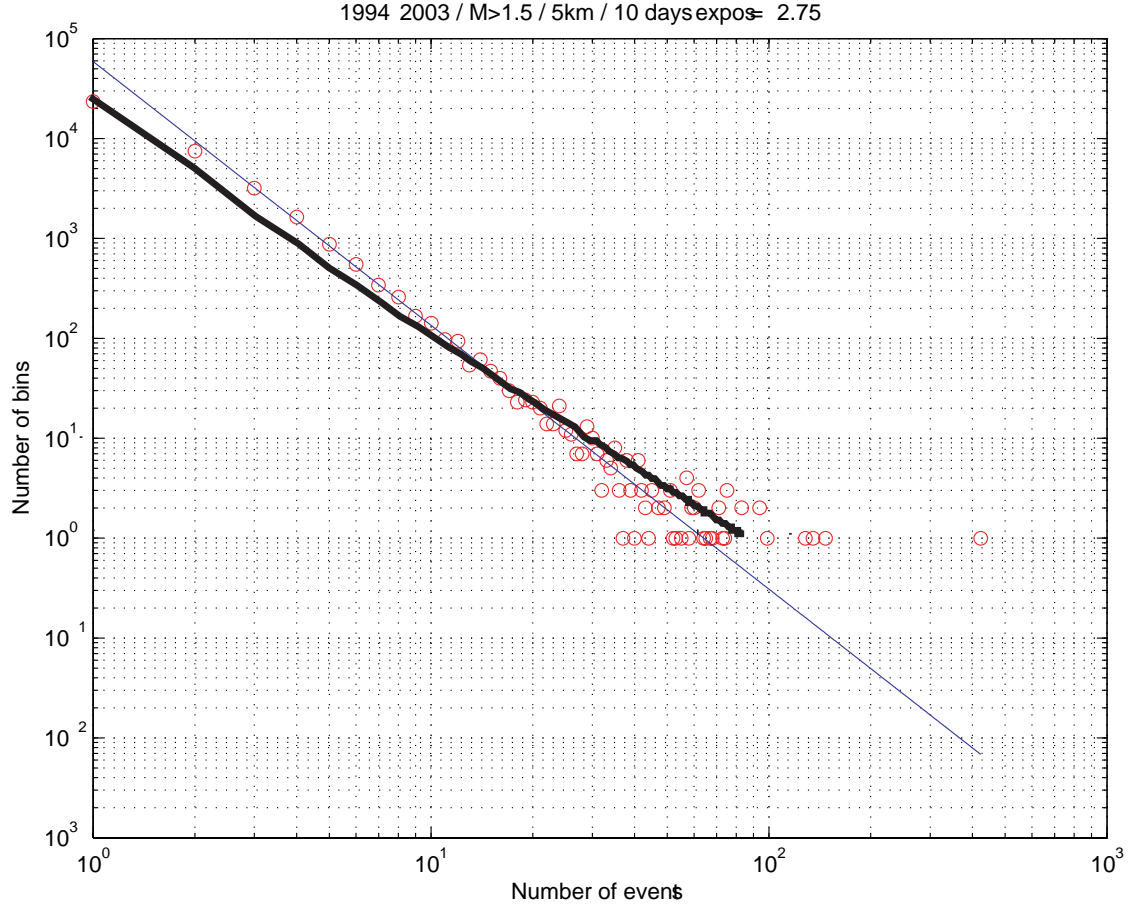


Fig. 9: Empirical probability density functions $P_{\text{data}}(r)$ of the number r of earthquakes in the space-time bins of size $5 \times 5 \text{ km}^2$ and $dt = 10$ days. The straight line is the best fit with a pure power law $P_{\text{data}}(r) \sim 1/r^{1+\mu}$ over the range $10 \leq r \leq 100$, which gives $\mu = 1.75$. The continuous line is the theoretical prediction using formula (110) with $dt = 10$ days and with no adjustable parameters, as the parameters are fixed to the values adjusted from the fit in Fig.7.

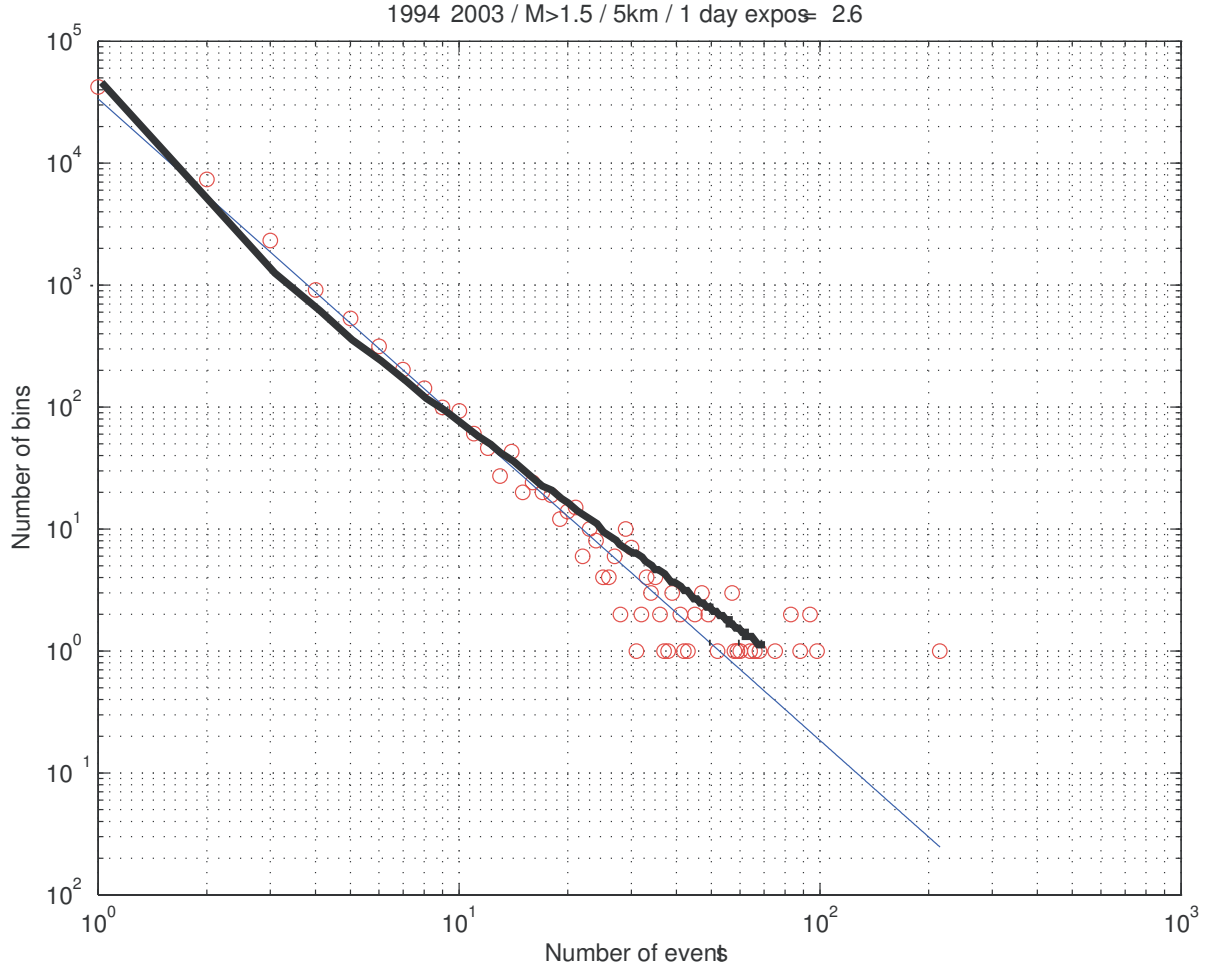


Fig. 10: Empirical probability density functions $P_{\text{data}}(r)$ of the number r of earthquakes in the space-time bins of size $5 \times 5 \text{ km}^2$ and $dt = 1$ day. The straight line is the best fit with a pure power law $P_{\text{data}}(r) \sim 1/r^{1+\mu}$ over the range $10 \leq r \leq 100$, which gives $\mu = 1.60$. The continuous line is the theoretical prediction using formula (110) with $dt = 1$ day and with no adjustable parameters, as the parameters are fixed to the values adjusted from the fit in Fig.7.

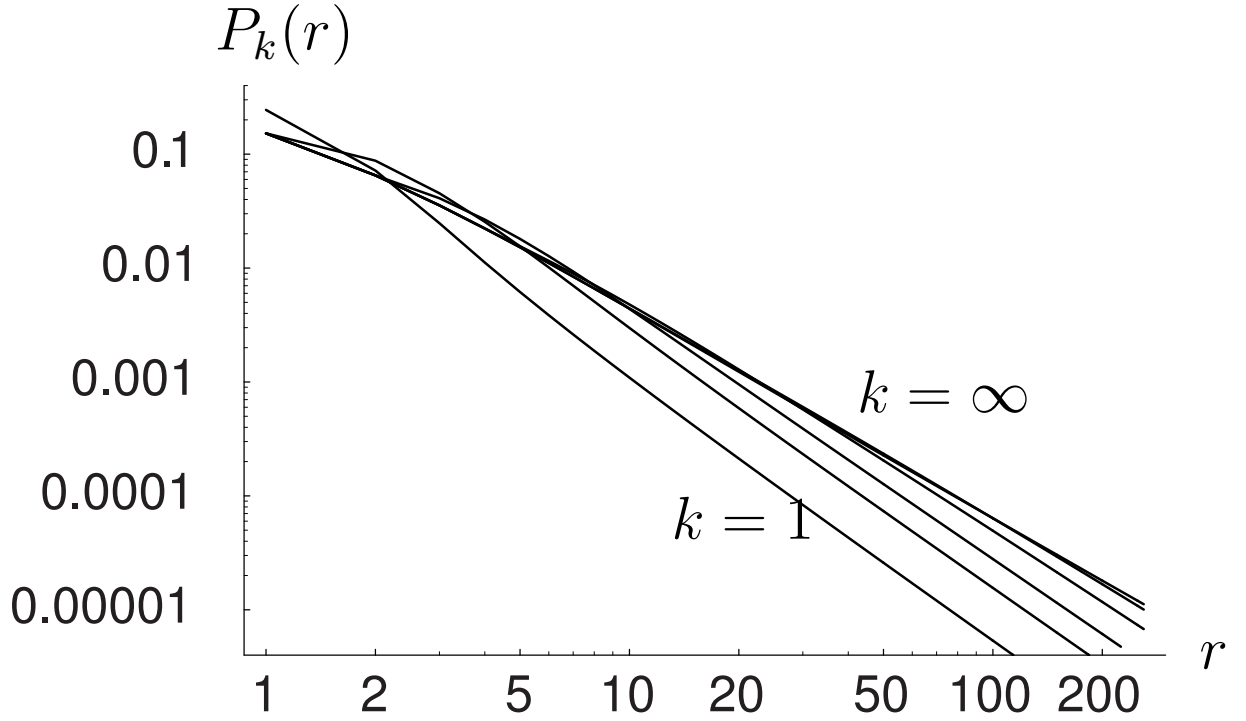


Fig. 11: Distributions $P_k(r)$ given by (113) for $\gamma = 1.25$, $n = 1$, for different numbers of generations $k = 1; 2; 3; 5; 8$. The upper curve corresponds to asymptotic distribution $P(r)$ given (114) corresponding to $k \rightarrow +\infty$, while lower one corresponds to the distribution $P_1(r)$ given by (18) of the number of aftershocks of first generation.

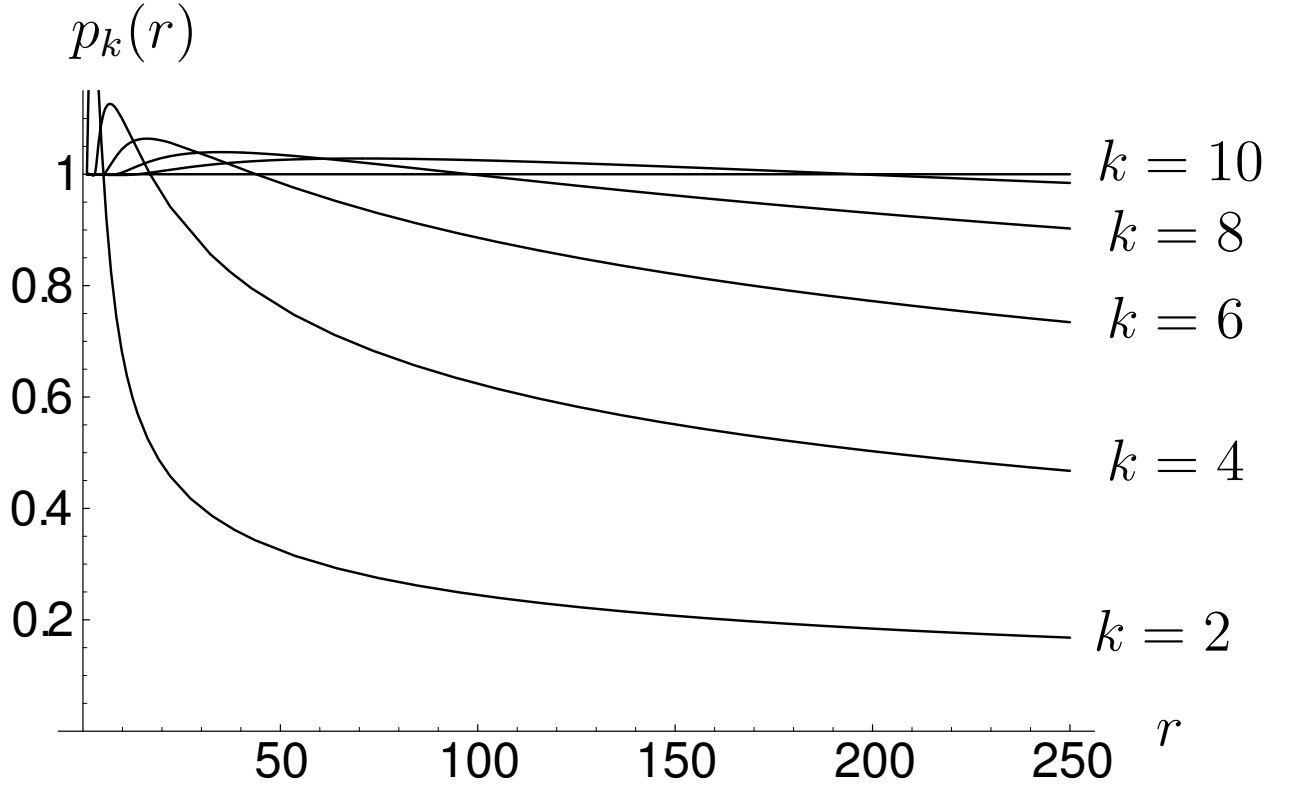


Fig. 12: Ratios (115) as a function of event numbers r for different values of the generation number k , demonstrating the convergence of the distributions $P_k(r)$ to the asymptotic distribution $P(r)$. Bottom to top: $k = 2; 4; 6; 8; 10$.

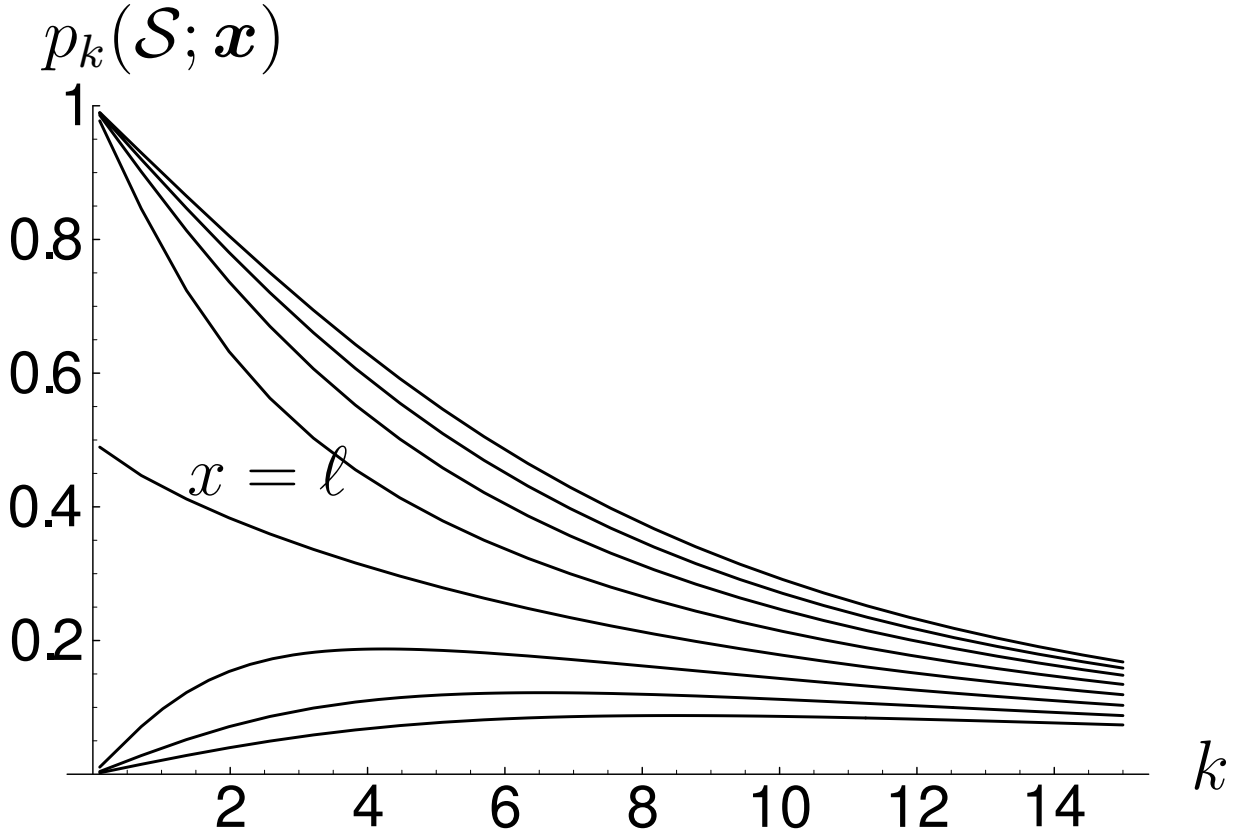


Fig. 13: Plots of the probabilities $P_k(r, \mathcal{S}; \mathbf{x})$ given by (132) for $\gamma = 1.25$, $n = 0.99$, $\ell = 10d$ and for different positions of the mother earthquake: $x/\ell = 0; 0.4; 0.6; 0.8; 1; 1.2; 1.4; 1.6$. Recall that ℓ is the radius of the assumed circular domain \mathcal{S} centered on the origin. The two families of curves separated by the central one for $x/\ell = 1$ are explained in the text.

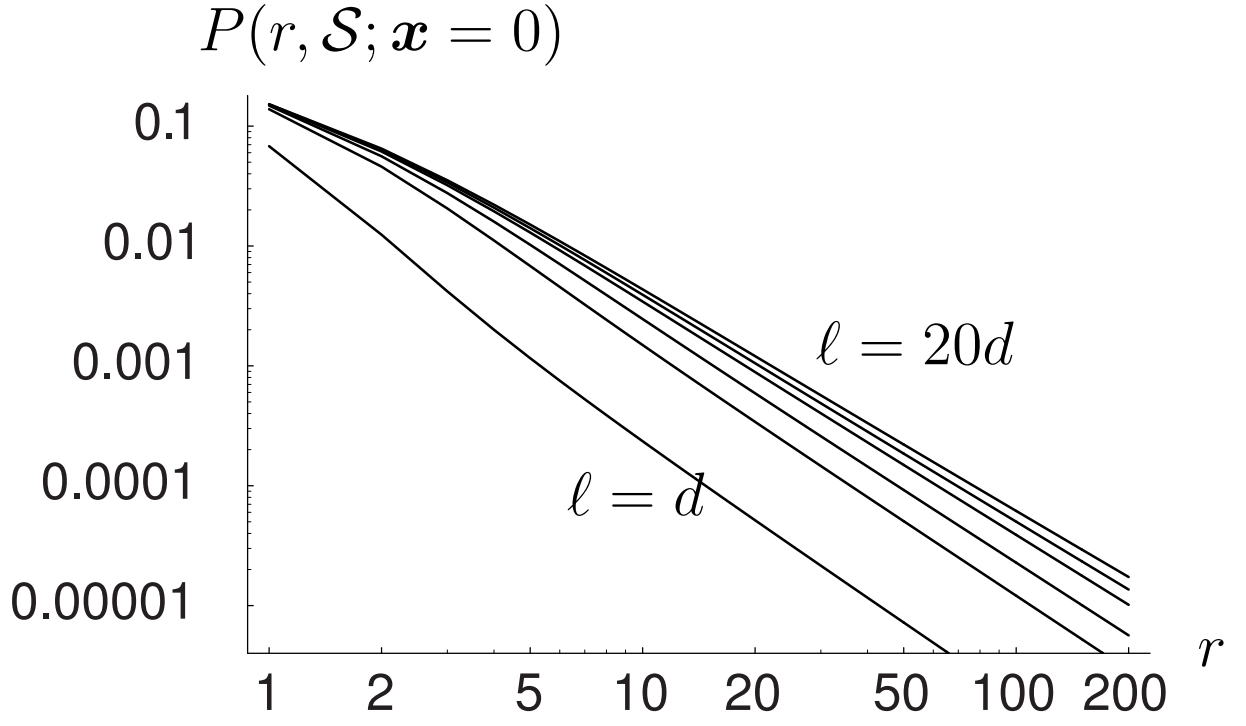


Fig. 14: Plots of the distribution $P(r, \mathcal{S}; \mathbf{x})$ of the total number r of aftershocks falling within the disk \mathcal{S} for a mother earthquake at the origin $\mathbf{x} = 0$ and for different values of the circle radius ℓ . Bottom to top: $\ell/d = 1; 3; 5; 10; 20$.

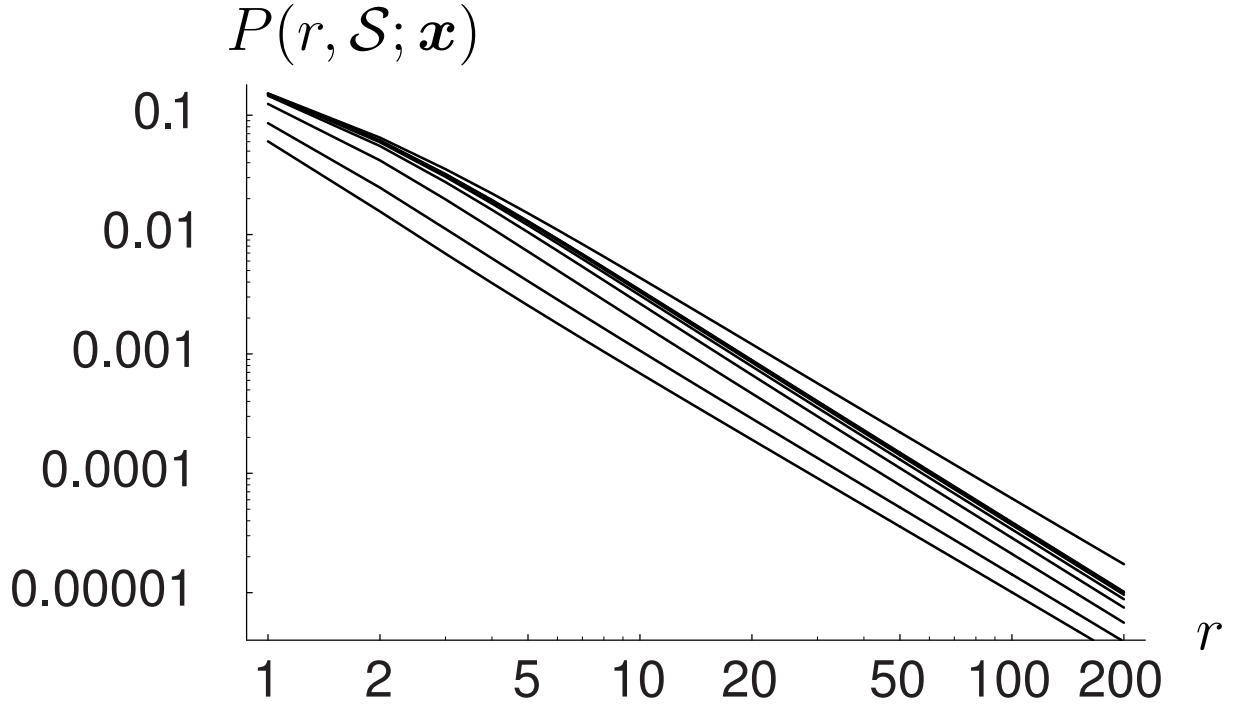


Fig. 15: Plots of the distribution $P(r, \mathcal{S}; \boldsymbol{x})$ of the total number r of aftershocks falling within the disk \mathcal{S} for different positions \boldsymbol{x} of the mother earthquake at fixed disk radius $\ell/d = 10$. Bottom to top: $x/\ell = 1.4; 1.2; 1; 0.8; 0.6; 0.4; 0.2; 0$. The upper curve thus corresponds to an infinite disk $\ell = +\infty$.

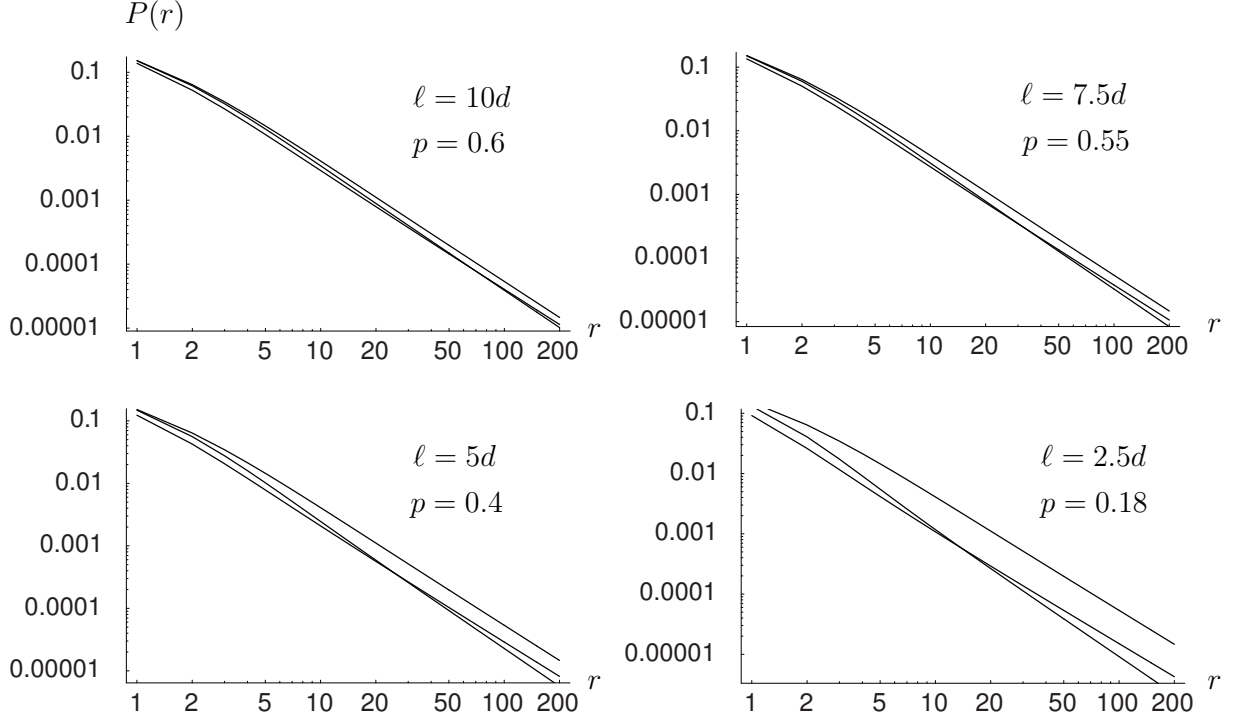


Fig. 16: Comparison of the asymptotic distribution $P(r, \mathcal{S}, \mathbf{x} = 0)$, obtained by calculating the integral (130) for a large enough generation number k ($k = 25$ is found to be sufficient), with the factorization approximation $P(r, p)$ given by (135), where $p = p_{\mathcal{S}}$ is defined as the fraction of the aftershocks which fall into the domain \mathcal{S} . The upper curve in each panel is the distribution (114) for an infinite domain $\ell/d = +\infty$, as a reference. The different panels correspond to $\ell/d = 10; 7.5; 5; 2.5$, with $\gamma = 1.25$, $n = 0.99$, $\mathbf{x} = 0$.